CHITOSAN BASED IN ELECTRON TRANSPORT LAYER (ETL) FOR PEROVSKITE SOLAR CELL (PSC)

NUR HIDAYAH SYAHIRA BINTI MOHD SATAR

UNIVERSITI TEKNIKAL MALAYSIA MELAKA

CHITOSAN BASED IN ELECTRON TRANSPORT LAYER (ETL) FOR PEROVSKITE SOLAR CELL (PSC)

NUR HIDAYAH SYAHIRA BINTI MOHD SATAR

This report is submitted in partial fulfilment of the requirements for the degree of Bachelor of Electronic Engineering with Honours

Faculty of Electronic and Computer Engineering
Universiti Teknikal Malaysia Melaka

2023

DECLARATION

I declare that this report entitled “Chitosan Based in Electron Transport Layer (ETL) for Perovskite Solar Cell (PSCs)” is the result of my own work except for quotes as cited in the references.

Signature : …………………………………

Author : NUR HIDAYAH SYAHIRA BINTI MOHD SATAR

Date : 19 JANUARY 2023

APPROVAL

I hereby declare that I have read this thesis and in my opinion this thesis is sufficient in terms of scope and quality for the award of Bachelor of Electronic Engineering with Honours.

Signature : ....

Supervisor Name : TS. ZARINA BINTI BAHARUDIN ZAMANI

Date : 19 JANUARY 2023

DEDICATION

I dedicate this entire thesis to my family because they have always been there for me during my ups and downs and have supported me throughout the completion of this thesis. I also dedicate this thesis to my supervisor and co-supervisor who taught me that proficiency is not the most important aspect of finishing a project rather than diligence and enthusiasm are the pillars of success.

ABSTRACT

Perovskite Solar Cells (PSC) are a new phenomenon with high efficiency and have a simple fabrication process. PSC has a lengthy lifespan when compared to the other commercially available crystalline silicon solar cell. However, PSC is reported to have limited flexibility and a high testing cost, it is not fully equivalent to other commercialised solar cell. By varying the time and temperature to show their performance, structural, electrical conductivity, and optical properties, the synthetization of the chitosan from deacetylation process have been made. In this project, chitosan was synthesized from dried shrimp shell to be used at the electron transport layer (ETL) to analyse the performance of the perovskite solar cell. Particle size analyser, Fourier Transform Infrared Spectroscopy (FTIR) and 4-Probe testing were used to characterize the chitosan. A sample of white powder chitosan with the degree of deacetylation were obtained through FTIR spectra. Chitosan with the highest percentage of the degree of deacetylation was used to mix with graphene and zinc oxide. Through this mixture, the resistivity and resistance of the mixture achieved at 2.41k and 3.88k(ohm). Furthermore, a simulation of this PSC using OghmaNano software was also done by varying the electrical parameters. The highest efficiency of 5.86% with chitosan mixed with zinc oxide was obtained from this analysis.

ABSTRAK

Sel Suria Perovskite (PSC) adalah fenomena baharu dengan kecekapan tinggi dan mempunyai proses fabrikasi yang mudah. PSC mempunyai jangka hayat yang panjang jika dibandingkan dengan sel solar silikon kristal lain yang tersedia secara komersial. Walau bagaimanapun, PSC dilaporkan mempunyai fleksibiliti terhad dan kos ujian yang tinggi, ia tidak setara sepenuhnya dengan sel suria yang dikomersialkan yang lain. Dengan mengubah masa dan suhu untuk menunjukkan prestasi, struktur, kekonduksian elektrik dan sifat optiknya, sintesis kitosan daripada proses penyahetilasi telah dibuat. Dalam projek ini, kitosan telah disintesis daripada kulit udang kering untuk digunakan pada lapisan pengangkutan elektron (ETL) untuk menganalisis prestasi sel suria perovskit. Penganalisis saiz zarah, Fourier Transform Infrared Spectroscopy (FTIR) dan ujian 4-Probe digunakan untuk mencirikan kitosan. Satu sampel serbuk kitosan putih dengan tahap penyahetilasi diperoleh melalui spektrum FTIR. Kitosan dengan peratusan tertinggi tahap penyahetilasi digunakan untuk dicampur dengan graphene dan zink oksida. Melalui campuran ini, kerintangan dan rintangan campuran dicapai pada 2.41k dan 3.88k(ohm). Tambahan pula, simulasi PSC ini menggunakan perisian OghmaNano juga dilakukan dengan mempelbagaikan parameter elektrik. Kecekapan tertinggi iaitu 5.86% dengan kitosan bercampur dengan zink oksida diperoleh daripada analisis ini.

ACKNOWLEDGEMENTS

First and foremost, I want to express my gratitude to Allah (SWT) for giving me all I needed to do this endeavor. I gave this project my all. However, this project would not have been able to succeed without the kind help and support of several people. I would like to sincerely thank each and every one of them.

Next, I would like to extend my sincere gratitude to my supervisor, Ts. Zarina Binti Baharudin Zamani and my co-supervisor, Dr. Muhammad Idzdihar Bin Idris, who have guided me through every stage of my project work and never ceased motivating me to complete my project.

Last but not least, I want to extend my sincere gratitude to my family and friends for their patience, encouragement, and practical support as I wrote my report from beginning to conclusion.

TABLE OF CONTENTS

LIST OF FIGURES

LIST OF TABLES

LIST OF SYMBOLS AND ABBREVIATIONS

PV : Photovoltaic Device

PSC : Perovskites Solar Cell

PCE : Power Conversion Efficiency

GO : Graphene Oxide

DOE : Design of Experiment

CO_2 : Carbon Dioxide

Si : Silicon

CIGS : Copper Indium Gallium Selenide

CdTe : Cadmium Telluride

TCO : Transparent Conductive Oxides

ITO : Indium Tin Oxide

FTO : Fluorine-doped Tin Oxide

HTM : Hole Transporting Material

TiO_2 : Tin Oxide

ZnO : Zinc Oxide

Au : Gold

Ag : Silver

Voc : Open Circuit Voltage

FF : Fill Factor

Jsc : Short Circuit Density

GO : Graphene Oxide

IPA : Isopropyl Alcohol

FTIR : Fourier-Transform Infrared Spectroscopy

UV-Vis : Ultraviolet-Visible Spectroscopy

PSA : Particle Size Analyzer

XRD : X-Ray Diffraction

SEM : Scanning Electron Microscope

HCL : Hydrochloric Acid

NaOH : Sodium Hydroxide

DA : Degree of Deacetylation

SDG : Sustainable Development Goals

LIST OF APPENDICES

CHAPTER 1

INTRODUCTION

This chapter will briefly describe the project introduction, objectives, problem statement, scope of work and also thesis structure. In this chapter will be introduce about the project background of a perovskite solar cell and green technology of polymer.

1.1 Project Background

In order to convert solar energy into usable electricity, a semi-conductor device called a solar cell is used. Silicon is used in solar cell because of its ability to absorb the sun's rays. This method was first identified in the early 1800s, but the first solar cell was not manufactured until 1954 by Bell[1]. Solar power has the capacity to grow and meet future energy demands. Recent years have seen a lot of research and development into photovoltaic (PV) devices, which quickly respond to changes in ambient circumstances and have a high-power conversion efficiency. A photovoltaic cell is a type of electronic device that uses the photovoltaic effect to directly convert light energy into electricity. All photovoltaic cells convert light energy into electricity using semiconductors, the substances that lie between electrical insulators like glass and metallic conductors like copper. Photovoltaic cells, an established technology for producing solar energy, have seen tremendous growth during the past ten years[2].

The first generation of solar cells are created using thin-film solar panels, mono-crystalline silicon crystals, poly-crystalline silicon crystals, and silicon wafers. The most recent and promising generation of solar cells includes concentrated solar cells, polymer-based solar cells, dye-sensitized solar cells, nanocrystal-based solar cells, and perovskite-based solar cells[1].

Green technology, often known as "green-tech" or "green technology," is a relatively young field of study that focuses on creating environmentally friendly technologies in an effort to lessen the negative effects that humans have on the natural world[1]. Energy, atmospheric science, agriculture, materials science, and hydrology are only some of the many scientific fields that contribute to green technology. Green technology has many benefits, including being environmentally friendly which emitting no harmful gases into the atmosphere, being inexpensive to run, never running out lowering atmospheric concentrations of carbon dioxide (CO_2), and mitigating the effects of global warming [3]. Figure below show the differences between conventional and renewable energy.

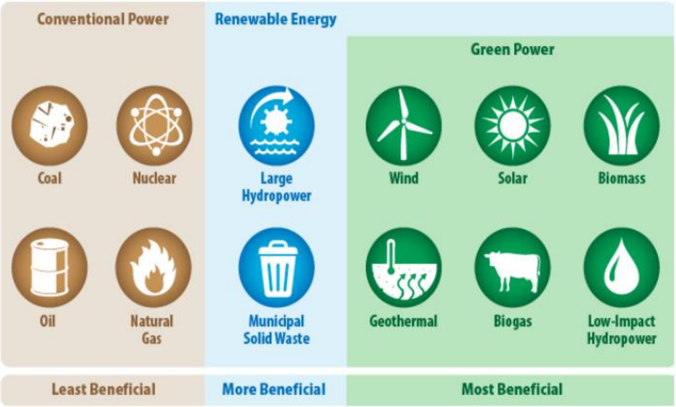

Figure 1.1: Definition of green power based on its relative environmental benefits[3].

1.1.1 Perovskite Solar Cell

Semiconductor materials have their electrons excited by sunlight, leading to electron flow into conducting electrodes and the generation of electric current. Perovskite solar cell (PSC) are highly sought after as a potential cost-effective and simple-to-manufacture component of the next generation of photovoltaic technology [4]. Changing or changing the solar cell's parameter might increase its efficiency as a PSC. Some examples of PSCs are the printed triple mesoscopic structure, as well as the mesoscopic formal (n-i-p) and inverted (p-i-n) structures same as figure 1.2 below.

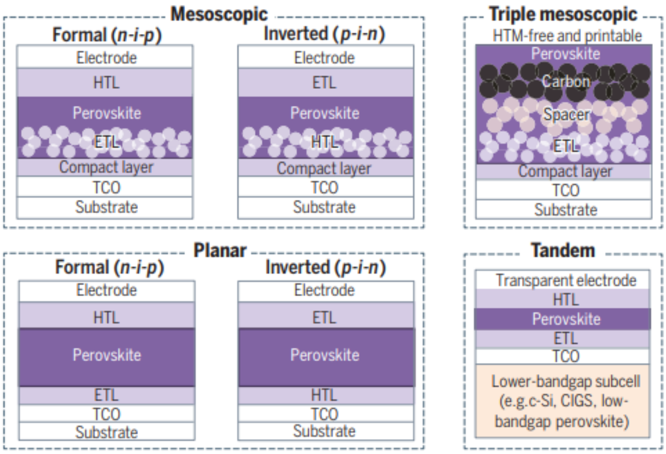

Figure 1.2: Configurations and Application Demonstration of PSC[4].

1.1.2 Chitosan

Chitosan is produced by N-deacetylating N-acetyl chitin. Chitosan is used in the food and bioengineering industries for a variety of purposes, including as the immobilization of enzymes, the controlled delivery of pharmaceuticals, and the stimulation of plant growth in agriculture[5]. Chitosan acts as an antibacterial and a defense elicitor. Chitosan's biodegradability, biocompatibility, bioactivity, non-toxicity, and polycation characteristics are all noteworthy. The physicochemical and structural features of chitosan are described in this work.

However, chitosan-based additives are expected to boost its efficiency even more by facilitating the binding of additional electrodes to the PSC photoanode. Several trial synthesis of nanoparticles were conducted to investigate and identify the growth of graphene oxide (GO) combined with the chitosan based. The method established by other researchers for synthesizing chitosan can be used. Numerous techniques can be used to examine the experiment's findings, and visuals of the samples can be viewed for inspection. This PSCs production process requires the following steps: paste preparation, glass deposition, counter electrode preparation, PSC synthesis, and performance analysis. Therefore, the Design of Experiment (DOE) serves as the analytical framework for this study's linking of the flow process and its outcomes.

1.2 Problem Statement

Due to its excellent conversion efficiency with validated PCE and the potential to cut costs and simplify the fabrication process, PSC has drawn attention among next-generation solar technologies. The stability of PSC has been a major area of focus in recent years, and it has made significant progress. PSC has recently exhibited a lifetime of 10,000 hours under 1 sun (1kW/m2) lighting with a UV filter at a steady temperature as high as 55°C and under short-circuit conditions [4]. This radiation is equivalent to what most of Europe would receive from 10 years of outdoor use. To develop uniform testing standards across the PSC community, further work must be done. By providing both initial photovoltaics, it is also possible to improve the openness of reporting requirements for stability testing. For the current PSC, the key challenges include low flexibility and a costly production process.

Due to the conflict between fulfilling optical and electrical criteria for light collection and current extraction, the majority of thin-film solar cells have low power conversion efficiency. As opposed to non-crystalline thin film cells, crystalline media has a higher energy conversion efficiency, which is why the vast majority of PV cells on the market today employ it. Crystalline silicon, the most common component, has low optical absorption and necessitates a moderately thick layer (200m) to effectively gather light[6].

The shrimp processing sector is especially popular in coastal areas. Only the meat is used in the processing; the head and shell are thrown away. An estimated 80,000 tons of garbage are generated annually in the fish sector [5]. Due to the enormous volume of waste, degradation is a sluggish process, leading to waste accumulation over time. Recycling shell waste into economically viable materials like chitin is an easy and practical way to reduce this environmental issue.

1.3 Objectives

There are a few goals for this project that must be met. The following is a list of this project's goals:

i. To synthesize the chitosan from shrimp shell by deacetylation process.
ii. To analyze the performance, structural, electrical and optical properties of thin layer chitosan mixed with graphene and zinc oxide.
iii. To simulate chitosan mixed with graphene and zinc oxide as Electron Transport Layer (ETL) in inverted solar cell by using OghmaNano.

1.4 Scope of Works

The aim of this work is wish to center around the understanding of Perovskite Solar Cell’s layer, principle and attributes. The solar cell fabrication by employing chitosan as the based mixed with graphene and zinc is formed on electron transporting layer (ETL). The chitosan will be synthesized using the shrimp shell as the starting material. This work focuses on the production and analysis of mixed graphene oxide and zinc oxide with chitosan that operate as a PSCs based on their structure, features, electrical properties, and energy conversion efficiency.

1.5 Thesis Structure

In this structure, there will be five chapters to describe the project flow which is the fabrication between chitosan based, graphene and zinc for Perovskite Solar Cell. The chapters in the thesis will be as follows: Introduction, Literature Review, Methodology, Result, Discussion, and Conclusion.

Chapter 1 - This chapter discussed the background of the study, problem statement, objectives, and scope of work of the project.

Chapter 2 - This chapter consists of the background study and research about this project before fabrication. Besides, the background study contains the fundamental of the Perovskite Solar Cell, chitosan and previous works and journals that related to this project.

Chapter 3 - This chapter involved the process employed during the project development in methodology part, including the equipment, materials used and fabrication procedures for the Perovskite Solar Cell.

Chapter 4 - This chapter will explain detail about the result and discussion as well as analysis of the project after the fabrication process is done. Moreover, the electrical characteristic of Perovskite Solar Cell and calculation of the efficiency will also be defined.

Chapter 5 - This is the last chapter which is the conclusion of this project. The conclusion consists of the summary and recommendation for a better future development of this project.

CHAPTER 2

BACKGROUND STUDY

The Background Study chapter’s purpose is to extend upon the context and literature review of the project. It contains the project's information accumulation in order to complete the entire project. Research in books, newspaper, journals and articles are used in this chapter.

2.1 Solar Cell

For the sake of human civilization's long-term prosperity, solar cell hold great promise as a revolutionary new source of renewable energy. Solar is a safer and greener investment for the household and business. By using solar, it can quickly cut the electricity bill while provide energy independence in the face of growing energy bills and rising carbon dioxide (CO_2) emissions, and raise the value of that home or building. Today, solar energy is available.

Through a process known as the photovoltaic effect, sunlight can be transformed into electrical energy in solar cells. Since the Becquerel discovered the first photovoltaic effect in 1839, solar energy has been a scientific goal [7]. Every hour, Earth's atmosphere takes in enough solar energy to power the entire planet for a full year. Since the world cannot continue to rely solely on fossil fuels, research into the most efficient and economical solar cell has increased recently. PV technology is genuinely a sustainable and eco-friendly way to generate electricity [7]. PV technology has a wide range of advantages. The sun's energy is a limitless supply that can be harnessed in any part of the planet. Figure 2.1 shown that the solar radiation spectrum from wavelength 250 to 2500nm which include UV, visible and infrared spectral.

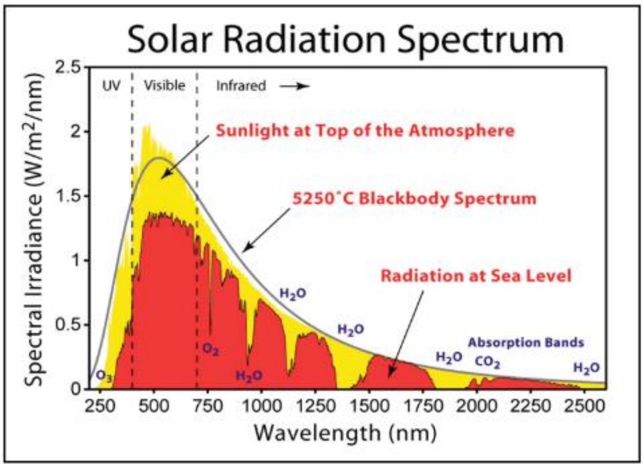

Figure 2.1: Solar irradiation spectrum at the surface and above the atmosphere [7].

Solar cells can only function if they can take in energy from the sun. Since more than 95% of the solar spectrum's irradiance falls between 250nm and 2500nm for Air Mass (AM) 0, the solar cell should try to absorb as much light as it can in the visible region of the spectrum (400-700nm) [7]. Using a single bandgap p-n junction, the cell's ultimate efficiency is projected to be roughly 49% at AM 1.5G. The efficiency of a single p-n junction solar cell was calculated using the detailed balancing concept by Shockley and Queasier (S-Q)[8]. It was determined that under one solar situation, the greatest efficiency was 30% for 1.1eV.

2.1.1 Generation of Solar Cell

Monocrystalline and multi-crystalline silicon (Si) solar cell are part of the first generation[8]. This generation has recently captured more than 90% of the market share. Due to its exceptional qualities, including non-toxicity, abundance, continuous efficiency, and sophisticated production capabilities, silicon has been a favoured choice for PV applications. Even though Si's bandgap is less than optimal for single junction cells, auger recombination significantly reduces the efficiency of these devices under full sun intensity.

The first silicon solar cell was developed by Bell Laboratories in 1954[7], with an efficiency of 6%. Silicon is still the most efficient material for home solar panels, with over 80% of all panels sold worldwide using the earliest commercial silicon conventional solar cell. Since silicon is the second most common element on Earth after oxygen, single-cell silicon photovoltaic systems are the most effective. It is a semiconductor material ideal for solar applications with a 1.1 eV [8] energy band gap.

They belong to the second generation of solar cells, which also comprise amorphous silicon (a-Si), copper indium gallium selenide (CIGS), and cadmium telluride (CdTe)-based thin film solar cells [8]. Amorphous silicon has traditionally been used to create thin-film solar cells. In comparison to CdTe solar cells, which now make up the majority of sales of thin-film solar cells, CIGS solar cells are believed to have a higher yield and a shorter payback period in terms of installed kWh/KWp. Because of its stability, high absorbability, and variety of manufacturing techniques, it is a top contender in the thin film industry. Figure 2.2 show the subset of solar cell which include polycrystalline, polymer solar cell, dye-sensitized solar cell and many more.

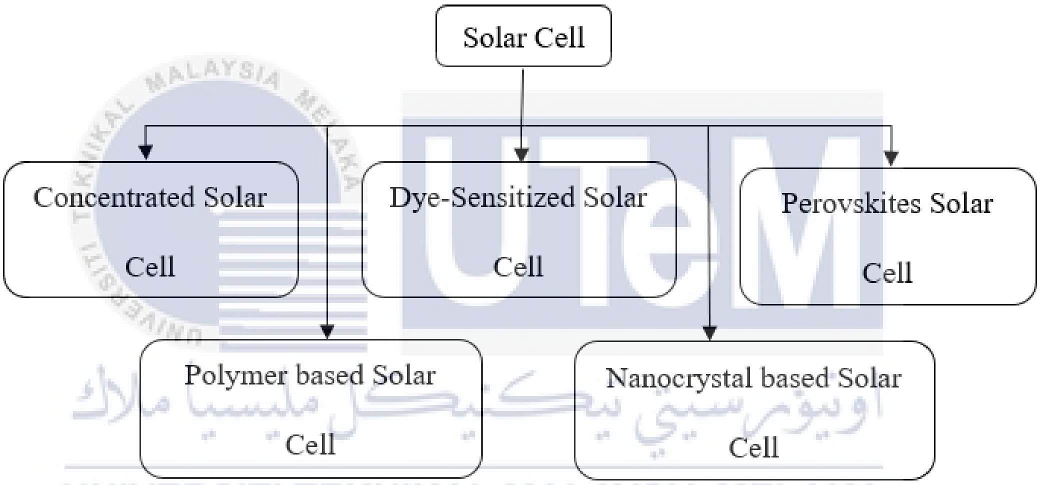

Figure 2.2: The third generation of solar cells[1].

The availability of a wide range of non-toxic and inexpensive materials, as well as the ease of manufacture, is a major factor in considering organic cell technology. However, despite the fact that polymer materials are relatively inexpensive, the cost-effectiveness has not yet been proven.

A substance or material known as a plasticizer is used to increase the flexibility, workability, or distensibility of a material that is frequently referred to as a plastic or elastomer. These substances reduce polymer deformation stress, hardness, density, viscosity, and electrostatic charge while increasing polymer chain flexibility, fracture resistance, and dielectric constant [9]. ITO's processing, encapsulation, and mirrors all greatly raise the price. The dyes employed in dye-sensitized solar cells have easier-to-produce PV characteristics and don't require the utilization of pricy, complicated machinery. Perovskite solar cells come in two varieties which is programmable bandgaps and fixed bandgaps [8]. They have various peculiar properties, including long s-orbitals and perovskite symmetry. Table 2.1 below shows each generation of solar cell include 1st generation, 2nd generation and the new generation of solar cell which 3rd generation.

Table 2.1: Generation of Solar Cell[1][8]

Generation of Solar Cell	
1st Generation	• Monocrystalline (Mono c-Si) • Polycrystalline (Poly c-Si) • Amorphous Silicon Cells • Hybrid Silicon
2nd Generation	• Amorphous Silicon (a-Si) • Cadmium Telluride (Cd-Te) • Copper-Indium-Selenide (CIS) • Copper-Indium-Gallium-Selenide (CIGS)
3rd Generation	• Dye-Sensitized (DSSC) • Perovskite (PSC) • Organic (OPV) • Quantum Dot (QD) • Kesterite solar cell

2.1.2 Efficiency of Solar Cell

The efficiency of solar cell is a limiting element in solar cell engineering. A fresh study on the efficiency of solar cell will be published every year. Individually measured findings are the most important condition for inclusion in the Figure 2.3 below, which is specified elsewhere.

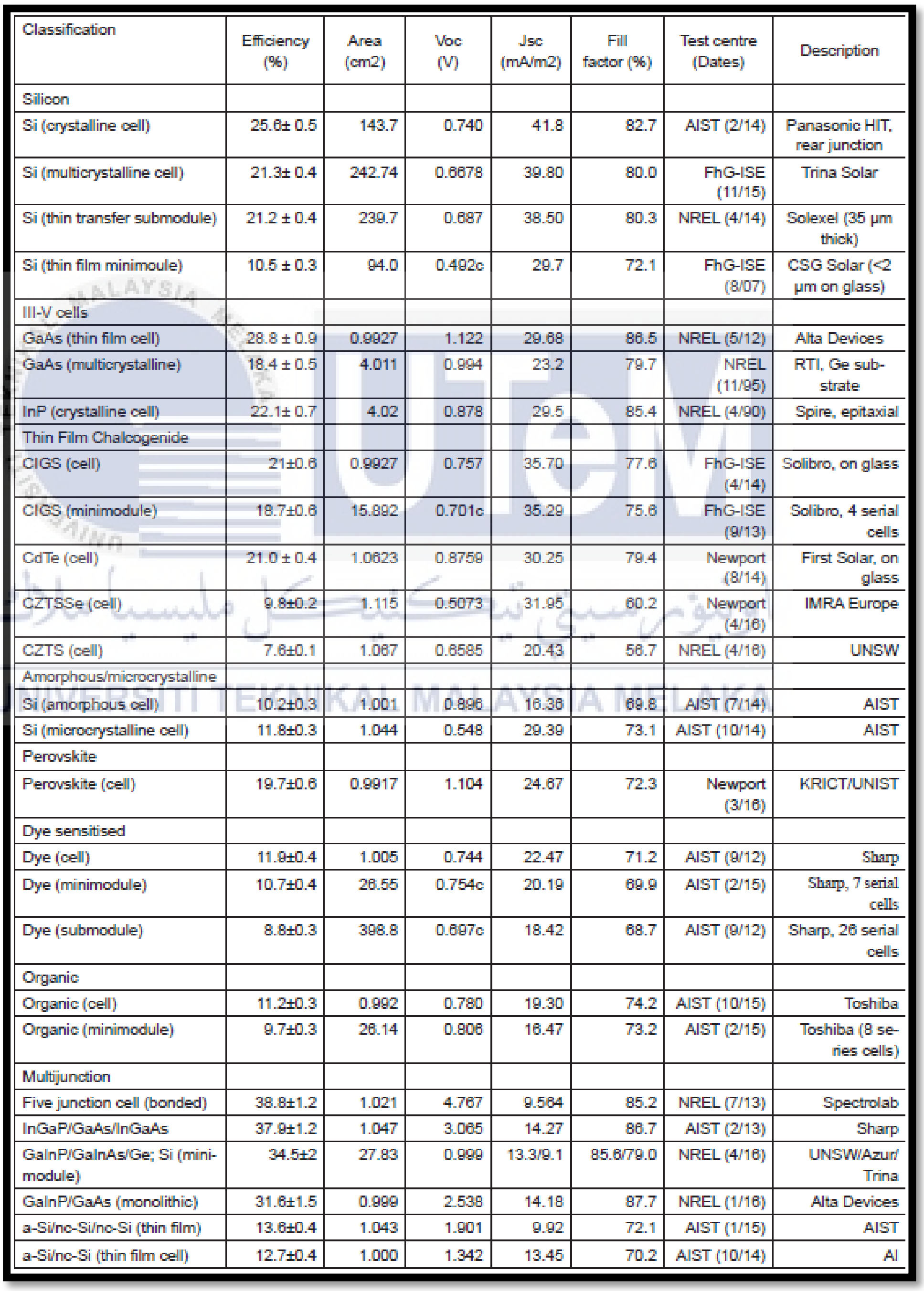

Classification	Efficiency (%)	Area (cm2)	Voc (V)	Jsc (mA/m2)	Fill factor (%)	Test centre (Dates)	Description
Silicon							
Si (crystalline cell)	25.6± 0.5	143.7	0.740	41.8	82.7	AIST (2/14)	Panasonic HIT, rear junction
Si (multicrystalline cell)	21.3± 0.4	242.74	0.6678	39.80	80.0	FhG-ISE (11/15)	Trina Solar
Si (thin transfer submodule)	21.2 ± 0.4	239.7	0.687	38.50	80.3	NREL (4/14)	Solexel (35 µm thick)
Si (thin film minimoule)	10.5 ± 0.3	94.0	0.492c	29.7	72.1	FhG-ISE (8/07)	CSG Solar (<2 µm on glass)
III-V cells							
GaAs (thin film cell)	28.8 ± 0.9	0.9927	1.122	29.68	86.5	NREL (5/12)	Alta Devices
GaAs (multicrystalline)	18.4 ± 0.5	4.011	0.994	23.2	79.7	NREL (11/95)	RTI, Ge sub-strate
InP (crystalline cell)	22.1± 0.7	4.02	0.878	29.5	85.4	NREL (4/90)	Spire, epitaxial
Thin Film Chalcogenide							
CIGS (cell)	21±0.6	0.9927	0.757	35.70	77.6	FhG-ISE (4/14)	Solibro, on glass
CIGS (minimodule)	18.7±0.6	15.892	0.701c	35.29	75.6	FhG-ISE (9/13)	Solibro, 4 serial cells
CdTe (cell)	21.0 ± 0.4	1.0623	0.8759	30.25	79.4	Newport (8/14)	First Solar, on glass
CZTSSe (cell)	9.8±0.2	1.115	0.5073	31.95	60.2	Newport (4/16)	IMRA Europe
CZTS (cell)	7.6±0.1	1.067	0.6585	20.43	56.7	NREL (4/16)	UNSW
Amorphous/microcrystalline							
Si (amorphous cell)	10.2±0.3	1.001	0.896	16.36	69.8	AIST (7/14)	AIST
Si (microcrystalline cell)	11.8±0.3	1.044	0.548	29.39	73.1	AIST (10/14)	AIST
Perovskite							
Perovskite (cell)	19.7±0.6	0.9917	1.104	24.67	72.3	Newport (3/16)	KRICT/UNIST
Dye sensitised							
Dye (cell)	11.9±0.4	1.005	0.744	22.47	71.2	AIST (9/12)	Sharp
Dye (minimodule)	10.7±0.4	26.55	0.754c	20.19	69.9	AIST (2/15)	Sharp, 7 serial cells
Dye (submodule)	8.8±0.3	398.8	0.697c	18.42	68.7	AIST (9/12)	Sharp, 26 serial cells
Organic							
Organic (cell)	11.2±0.3	0.992	0.780	19.30	74.2	AIST (10/15)	Toshiba
Organic (minimodule)	9.7±0.3	26.14	0.806	16.47	73.2	AIST (2/15)	Toshiba (8 series cells)
Multijunction							
Five junction cell (bonded)	38.8±1.2	1.021	4.767	9.564	85.2	NREL (7/13)	Spectrolab
InGaP/GaAs/InGaAs	37.9±1.2	1.047	3.065	14.27	86.7	AIST (2/13)	Sharp
GaInP/GaInAs/Ge; Si (mini-module)	34.5±2	27.83	0.999	13.3/9.1	85.6/79.0	NREL (4/16)	UNSW/Azur/ Trina
GaInP/GaAs (monolithic)	31.6±1.5	0.999	2.538	14.18	87.7	NREL (1/16)	Alta Devices
a-Si/nc-Si/nc-Si (thin film)	13.6±0.4	1.043	1.901	9.92	72.1	AIST (1/15)	AIST
a-Si/nc-Si (thin film cell)	12.7±0.4	1.000	1.342	13.45	70.2	AIST (10/14)	AI

Figure 2.3: Efficiencies of single-junction terrestrial cells and submodules estimated at 25°C under the global AM 1.5 spectrum (1000W/m^2)[7].

2.2 Perovskite Solar Cell

Due to the fact that organic–inorganic perovskites can transform from insulators to conductors by increasing the number of inorganic layers in their $(C_4H_9NH_3)_2$ $(CH_3NH_3)_{n+1}$ Sn_nI_{3n+1} layered perovskite, they have attracted interest [10]. This is an important discovery since these organic-inorganic perovskite compounds in [10] potentially yield high-temperature superconductors. As a result, the organic-inorganic halide perovskite materials' photovoltaic capabilities have not drawn much attention. Figure 2.4 shown that the differences type of solar cell structure that involved by different type of solar cell such as conventional solar cell structure, inverted solar cell structure and lastly mesoporous type of solar cell structure.

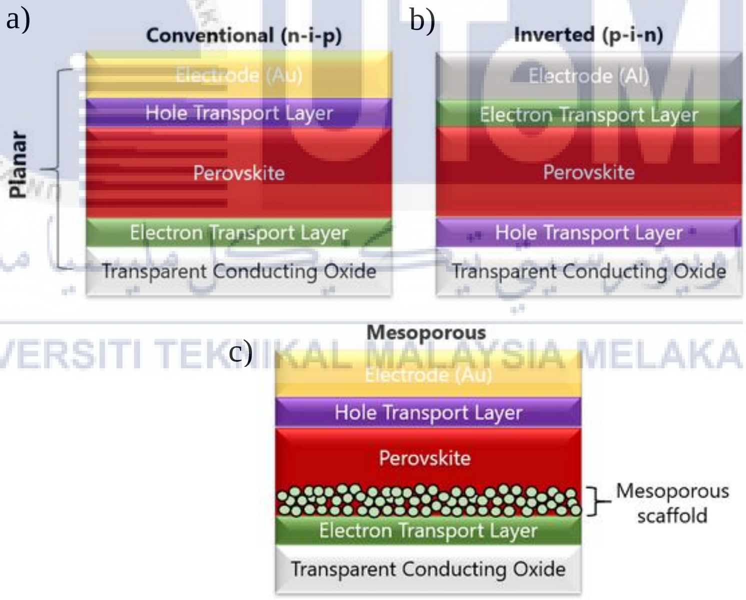

Figure 2.4: Perovskite Solar Cell Structure (a)Conventional (n-i-p), (b)Inverted (p-i-n), (c) Mesoporous

$CH_3NH_3PbX_3$ (X=Br and I) was initially tried in 2009 and employed as a semiconductor sensitizer in dye-sensitized liquid junction-type solar cell. Unlike common Ru-based molecular dyes, which have a power conversion efficiency (PCE) of greater than 11% [9] Our approach produced a PCE of 3-4% as opposed to semiconductor quantum dot sensitizers with PCEs of 5%–6%. The low solar performance and severe electrolyte instability of methylene ammonium lead halide perovskites have attracted little attention. Two years later, Park's team presented a $CH_3NH_3PbI_3$ perovskite solar cell with a 6.5% efficiency that was marginally more stable [9] in electrolytes than the previous cell.

2.2.1 Working Principle of Perovskite Solar Cell

Light harvester material has advanced significantly since Miyasaka's study, when she used it in a DSC setup that included nanostructured TiO2 perovskite sensitized solar cells. Since then, PCS have been developed using a variety of fabrication techniques, chemical compositions, and topologies, including Nano-heterojunction and planar thin film. The promising preliminary findings, with efficiency between 10-12% at one solar equivalent lighting, have quickly advanced to levels over 15% [10]. Using $CH_3NH_3PbI_3$ perovskite generated by a sequential solution approach on nanostructured TiO_2 as in a typical DSC and a thin film configuration using $CH_3NH_3PbI_{3-x}Cl_x$ created by vapor deposition, these record efficiencies have been recorded in two separate ways. Perovskite solar cell have been able to operate efficiently using a variety of different methods [9], which suggests that a robust photovoltaic operating mechanism is at work. As shown on the Figure 2.5 (a) below, is the normally structure of perovskite solar cell which consists of 5 layer from ITO glass, hole transport layer, perovskite compound, electron transport layer and metal electrode on top of it meanwhile, Figure 2.5 (b) shows that graph for open circuit which voltage respect to the Jsc(mA/cm^2).

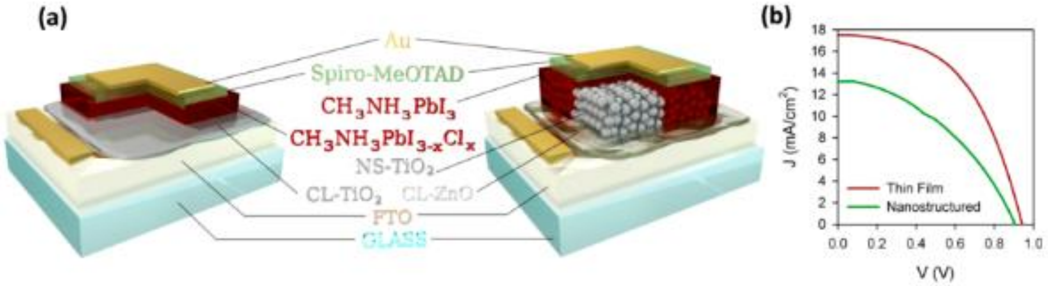

Figure 2.5: Solar cell configuration and performance [10] **(a) Perovskite Solar Cell structure, (b) Short-Circuit Graph**

PSCs with a mesoporous TiO_2 layer are the most frequent architecture. There is a fluorine-doped tin oxide (FTO), an n-type compact or blocking TiO_2, a mesoporous layer like TiO_2 or ZnO, a perovskite absorber layer, and a metal electrode like gold (Au) or silver (Ag) in a mesoscopic PSC. The basic operating principles start when light is absorbed by the perovskites in the perovskite layer, electrons are transferred to the electron-transfer layer (Figure 2.6c, step 2), while holes are transferred to the hole-transporting material (HTL; Figure 2.6c, step 3) and finally, these photogenerated charge carriers are collected at the front and back contacts of the solar cell. Recombination of photogenerated species (Figure 2.6(c), step 4) and back charge transfer mechanisms at the TiO_2/perovskite/HTL interfaces (Figure 2.6(c), steps (5)–7) are alternative charge transfer processes [11]. Electron–hole pair recombination is avoided by the mesoscopic structure, which provides an efficient diffusion length.

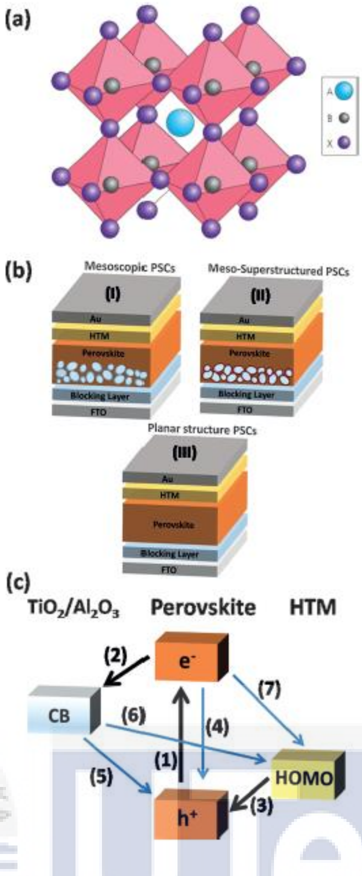

Figure 2.6: Perovskite crystal structure [11] **(a) Orthorhombic, (b) Cubic, (c)Tetragonal**

Meanwhile, Table 2.2 shown that the differences of each of the perovskite crystal structure depending on a few method used based on their theoretical lattice constants.

Table 2.2: The theoretical lattice constants of the $CH_3NH_3PbI_3$ data [11].

$CH_3NH_3PbI_3$	Method	a [A]	b [A]	c [A]	Volume [A^3]
Orthorhombic	PZ81/LDA	8.678	12.387	8.318	894.05
	PBE/GGA	9.226	12.876	8.619	1023.88
	OptB86b+vdWDF	8.831	12.648	8.570	957.18
Cubic	PBE	6.49	6.49	6.50	273.8
	PBE+vdW^{TS}	6.35	6.35	6.36	256.3
	PBE+vdW	6.35	6.35	6.35	255.9
Tetragonal	PBE	9.04	-	-	1056.4
	PBE+vdW^{TS}	8.89	-	-	1003.9

2.2.2 Component of Perovskite Solar Cell

The perovskite substance [13] is derived from the calcium titanite (CaTiO3) molecule and has a chemical structure of type ABX3. Perovskites' exceptional optical, thermal, and electromagnetic properties have generated a lot of interest, as have their cubic lattice-nested octahedral multilayer structures. Perovskite organic-inorganic metal halide compounds, which include perovskite solar cell materials, are a particular kind of organic-inorganic metal halide compound in which group A (methylammonium ($CH_3NH_3^+$) MA^+ or formamidine ($CH(NH_2)_2^+$, FA^+ is located in the vertex of the face-centered cubic lattice and the metal cation B such as Pb^{2+} and Sn^2. In the core and the apex of the octahedron, the anion X either Cl-, Br-, or I-, or a coexistence of many halogens is located [12].

Materials that have this kind of structure can be distinguished by four features. This is partly because of the materials' strong optical absorption coefficients, which can reach 104 cm^1, and their favorable photoelectric properties [14]. Perovskite can more efficiently collect solar energy since it is the layer that absorbs light. The materials are easily able to transport electrons and holes due to their high dielectric constant. Electrons and holes can be transferred simultaneously for distances of up to 100 nm [13] or much more and even more than 1 m.

2.3 Chitosan

In the chitin family, chitosan is an N-deacetylated type natural polymer. Using the deacetylation of chitin in the exoskeletons of crustaceans, fungi, and insects, chitosan is produced as a linear polysaccharide mostly composed of deacetylated units of D-glucosamine and N-acetyl-D-glucosamine [13]. Chitin and chitosan are polysaccharide s with fascinating intrinsic characteristics that can be processed rather easily. Additionally, these polymers have a fascinating surface that can be used for a variety of simple and complex applications. Many different applications for chitosan can be found, including molecular separation, food packaging film, prosthetic skin, bone substitutes, and water treatment [14]. Biomedical and environmental applications may be able to benefit from the development of environmentally friendly, easy-to-use and functional products that have been developed by a number of researchers in recent years.

2.3.1 Introduction to Chitosan

Chitosan is a byproduct of chitin, a natural chemical formed from the shells of crabs and shellfish. Chitin is used in the medical, health, electronics, and many more fields, as its biocompatibility has been demonstrated by science. The structure of chitosan is quite similar to that of cellulose, therefore it can be combined with cotton and viscose. As a linear copolymer, chitosan is made up of two different sugars, acetamido and acetyl, which are connected together by glyosidic bonds β(1→4) [15]. Insect and marine invertebrate exoskeletons include a carbohydrate known as chitin, which can be converted into chitosan through the N-deacetylation process of this polymer. Furthermore, chitosan is a biopolymer with a distinctive molecular structure, featuring reactive amino groups in its main chain, and high viscosity [16].

Chitin is the naturally occurring polysaccharide produced in vast amounts by living organisms on Earth. Its production is comparable to that of cellulose, which is produced organically by plants. As depicted in the Figure 2.7 below, (a) Chitin crystal structure and (b) Chitosan crystal structure have a chemical structure remarkably similar to that of (c) Cellulose crystal structure.

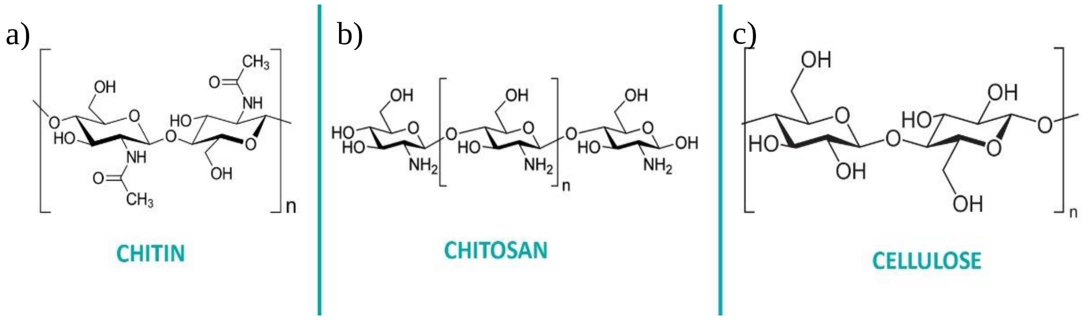

Figure 2.7: Chitosan crystal structure (a) Chitin, (b) Chitosan, (c) Cellulose

This white and pore-filled carbohydrate, chitin, is used to make the crustacean shells of crustaceans such as crabs, lobsters, and squid. Approximately 150'000 tons of Chitin is also accessible for commercial use each year, according to estimates [17]. Despite this, the world only uses a few thousand metric tons annually. Natural foods like crabs, shrimps, mushrooms, and chitin are all safe sources of chitin. It has been proven to be safe through numerous scientific studies. Remarkable for one's ability to perform well it is known that Chitin is abundantly produced organically on this planet and that it possesses a slew of beneficial characteristics [17].

2.4 Graphene

Graphene is a single layer of honeycomb-like graphite or carbon atoms. Also, it is one of the most promising nanomaterials ever identified. Graphene is the thinnest, strongest, and most electrical and thermally conductive material on the planet. Graphene's bonding enables for quicker electron mobility. Because of its mobility, graphene can be employed in both solar panels and hydrogen fuel cell technology.

A two-dimensional single-layered graphene, the basic building block for naturally occurring graphite, on the other hand, has recently gained a lot of attention, owing to its inexpensive cost, unusual structure, and amazing electrical and mechanical capabilities [18]. Graphene is an uncommon material, particularly for high-speed electronics. Graphene is believed to be unusual because to its one-of-a-kind high intrinsic carrier mobility, which can reach 200,000 cm2/Vs at room temperature [19]. Refer to the Table 2.3, these are the electrical properties of graphene after P. You simulated by using software.

Table 2.3 : Electrical Properties of Graphene [20]

	Graphene
Electron Mobility (cm^2/Vs)	210
Hole Mobility (cm^2/Vs)	9000
Voc (V)	0.905
Jsc (mA cm^{-2})	16.35
FF (%)	59.07
PCE (%)	8.74

Figure 2.8 below shown the result of their simulation consists of average for power conversion efficiency (PCE), voltage open circuit, current for short circuit, fill factor, power conversion efficiency for different top of graphene electrode from 1 - 4L.

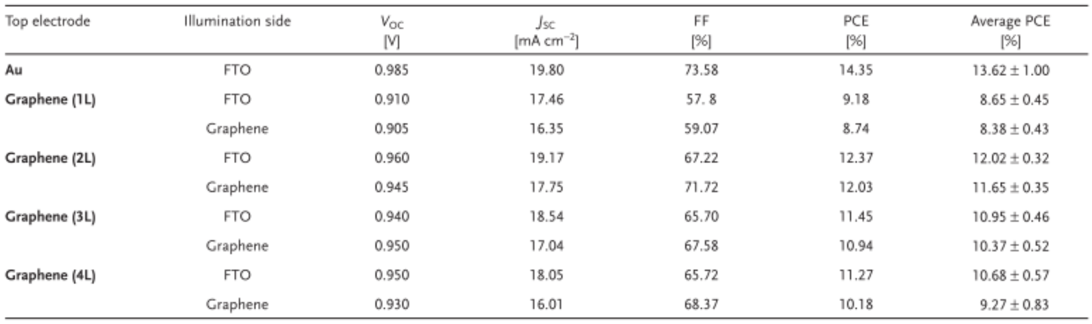

Top electrode	Illumination side	V_{OC} [V]	J_{SC} [mA cm^{-2}]	FF [%]	PCE [%]	Average PCE [%]
Au	FTO	0.985	19.80	73.58	14.35	13.62 ± 1.00
Graphene (1L)	FTO	0.910	17.46	57. 8	9.18	8.65 ± 0.45
	Graphene	0.905	16.35	59.07	8.74	8.38 ± 0.43
Graphene (2L)	FTO	0.960	19.17	67.22	12.37	12.02 ± 0.32
	Graphene	0.945	17.75	71.72	12.03	11.65 ± 0.35
Graphene (3L)	FTO	0.940	18.54	65.70	11.45	10.95 ± 0.46
	Graphene	0.950	17.04	67.58	10.94	10.37 ± 0.52
Graphene (4L)	FTO	0.950	18.05	65.72	11.27	10.68 ± 0.57
	Graphene	0.930	16.01	68.37	10.18	9.27 ± 0.83

Figure 2.8: Photovoltaic parameter of semi-transparent perovskite solar cell with Graphene[20]

2.5 Zinc Oxide

Zinc oxide (ZnO) is an inorganic compound. It comes in the shape of a white, soluble powder. Zinc oxide is used as an addition in a wide range of goods and materials, including cosmetics, nutritional supplements, rubber, plastics, ceramics, glass, cement, lubricants, paints, ointments, adhesives, sealants, pigments, meals, batteries, ferrites, and first-aid tapes. Although the mineral form of zincite does occur naturally, most zinc oxide is manufactured.

ZnO is a wide-band gap semiconductor that belongs to the II-VI semiconductor family. N-type doping happens naturally in semiconductors and is triggered by oxygen vacancies or zinc interstitials. Other desirable characteristics include good transparency, excellent electron mobility, a wide band gap, and strong room-temperature luminescence. Several emerging applications, including as transparent electrodes in liquid crystal displays, heat- or energy-efficient windows, and electronics like thin-film transistors and light-emitting diodes, benefit from ZnO's advantages due to these properties. Refer to the Table 2.4 below shown that these are the electrical properties of zinc oxide from running simulation of Scap1D software.

Table 2.4: Electrical Properties of Zinc Oxide

	Zinc Oxide
Electron Mobility (cm^2/Vs)	200
Hole Mobility (cm^2/Vs)	180
Dielectric Constant	8.5
Bandgap (eV)	3.4
Voc (V)	0.693
Jsc (mA/cm^{-2})	1.33
FF (%)	0.45
PCE (%)	0.63

2.6 Summary

No.	Title (Book/Journal)	Method	Finding
1.	Chitosan as biopolymer binder for graphene in supercapacitor electrode [**2021**]	• Surface morphology was inspected using scanning electron microscopy (SEM). • X-ray diffractometry (XRD) used to characterize the structure properties.	• Three best weight percentage of chitosan binder is 10 wt.%, leading to good homogeneity and bonding. • The fabrication of asymmetric supercapacitor (MnO2–graphene–chitosan//graphene–chitosan) has a decent energy density of 80.40 Wh kg− 1 at a power density of 2894.61 Wh kg− 1.
2.	Performance of Chitosan Based Polymer Electrolyte for Natural Dye Sensitized Solar Cell [**2018**]	• Chitosan based polymer electrolyte film was prepared by cast technique.	• Obtained solar cell conversion efficiency was about 1.8% with fill factor 53% using an irradiation of 100 mW/cm2 at 25˚C. • The prepared DSSC is not only stable but also eco-friendly due to use of natural polymer and dye.
3.	A review: Synthesis and applications of Graphene / Chitosan Nanocomposites [**2015**]	• Prepared PVA/CS/graphene composite nanofibers using aqueous electrospinning.	• The surface of GO still has many defects. • Discover more suitable polymers to combine with GO and obtain a more valuable nanomaterial.

4.	Deacetylation modification techniques of chitin and Chitosan [**2017**]	• Using deacetylation of Chitin to form chitosan. • Having 3 process which is demineralization, deproteinization and deacetylation.	• Partial deacetylation of chitosan where samples with a DDA of 45–55% display good solubility in weak acids due to protonation of the amino group. • Chitosan films with higher DDA improved tensile strength, elongation, and water transmission rates, and changes in the molecular arrangement structure in the film state of the chitosan.
5.	Semi-transparent Perovskite Solar Cells [**2020**]	• The use of solvent properties to form islands of perovskite using dewetting on the surface.	• The best solar cell using this method was fabricated with 30 wt. % perovskite solution, where the HC scaffold was formed with 600 nm PS and 8 min of plasma etching. • The results in a PCE of 10.3% and an AVT of 38%. • Thin films usually suffer from spectral losses due to insufficient light absorption.
6.	Perovskite Solar Cells: From Materials to Devices [**2014**]	• Deposit CH3NH3PbI3 Perovskite on a substrate, using two method that is, one-step and two-step coating methods.	• Optical absorption coefficient and thickness of the light absorber, the maximum efficiency for a 1 µm-thick perovskite solar cell composed of CH3NH3PbI3 is 26%.

			• Higher than the efficiency of a GaAs solar cell with the same thickness.
7.	Sustainable and eco-friendly strategies for shrimp shell valorization Gincy [**2020**]	• Optical absorption coefficient and thickness of the light absorber, the maximum efficiency for a 1 µm-thick perovskite solar cell composed of CH3NH3PbI3 is 26%. • Higher than the efficiency of a GaAs solar cell with the same thickness.	• Optical absorption coefficient and thickness of the light absorber, the maximum efficiency for a 1 µm-thick perovskite solar cell composed of CH3NH3PbI3 is 26%. • Higher than the efficiency of a GaAs solar cell with the same thickness.
8.	Perovskite-Based Solar Cells: Material, Methods and Future Perspective [**2017**]	• 3 types: the solution method, the vapor-deposition method, and the vapor-assisted solution method.	• A solution of the inorganic component is spin-coated on a substrate, subsequent spin-coating (or immersing) of a solution containing the organic component followed by annealing. • Less control over film thickness as compared to vacuum processes.
9.	Graphene/Metal Oxide Nanocomposite Usage as Photoanode in Dye-Sensitized and Perovskite Solar Cells [**2020**]	• Graphene nanoparticles were synthesized by modified Hummer’s method.	• PCE and DSSC was enhanced with the addition of graphene and optimum results found for 30wt% of graphene concentration.

10.	One-step synthesis of LaNiO3 with Chitosan for dry reforming of methane [**2018**]	• Doping or combining it with one-step synthesis using chitosan as a chelating agent.	• The catalytic tests were conducted at three temperatures: 600, 700 and 800C. • The results indicated the formation above 95% of LaNiO3 with good chemical homogeneity at lower temperature.
11.	Well-Dispersed Chitosan /Graphene Oxide Nanocomposites [**2010**]	• Prepared by the Hummer's method. • Simple self-assembly method by solution mixing. • CS/GO nanocomposites with 0.3, 0.5, and 1 wt.% of filler were prepared.	• The XPS spectra of CS/GO 1 wt.% nanocomposite display no obvious changes in the spectrum in comparison to CS. • The spectrum of CS, that of the CS/GO nanocomposite in 401.7 eV increase from 7.1% to 11.3%.
12.	Characterization and drug release performance of biodegradable chitosan–graphene oxide nanocomposites [**2014**]	• Polymer coated GO nanosheets use to improve the biocompatibility of GO. • Atomic force micro-scope (AFM) with Olympus AC160TS probes used to analyze the thickness and dimensions of GO sheets.	• CGO–0.5%, CGO–1% and CGO–5% do not strain soften after yielding but proceed straight to work hardening before failing. • Lower GO contents, 0.25 wt.%, are expected to lead to better dispersion and more efficient reinforcements. • The lower moduli exhibited by CGO–0.5% and CGO–1% nanocomposites can be attributable lower crystallinities. • CGO–5% shows the lowest modulus, presumable due to the presence of defects

			and aggregates in addition to the low crystallinity.
13.	Chitosan-Assisted Crystallization and Film Forming of Perovskite Crystals through Biomineralization [**2016**]	• Bioinspired synthesis used advanced materials by mimicking the biomineralization method.	• Application of chitosan resulted decrease in the perovskite crystal size with more uniform size distribution and smoother perovskite film.
14.	Effect of Polyethylene Glycol Incorporation in Electron Transport Layer on Photovoltaic Properties of Perovskite Solar Cells [**2020]**	• Synthesized ZnO sol by the sol–gel method.	• PEG effectively passivated the surface defects of ZnO, increased the electrical conductivity, and suppressed the charge recombination. • At 0.2 wt.% PEG incorporation, the PCE increased from 9.19 to 11.48%, an enhancement of 25%. • The photocurrent density could increase from 15.2 to 19.2 mA/cm2, an increase of 27%.
15.	Enhanced performance of planar perovskite solar cells using low-temperature processed Ga-doped TiO2 compact film as efficient electron-transport layer [**2018]**	• Fabricated by one-step method. • The annealing temperature of TiO2 electron-transport layer (ETL) set at 200 °C.	• The optimum Ga concentration, the PSCs based on Ga-TiO2 and ETL achieve the highest power conversion efficiency (PCE) of 17.09% and 14.63%, and an average PCE of 16.51% and 14.15%, respectively.

CHAPTER 3

METHODOLOGY

The methodology is strongly related to the rules and the use of a flow chart to depict the project's path. The Gantt chart can also be applied to all activities carried out during the course of the project. All of the implementation phases are used in this chapter, and the flow chart and Gantt chart are presented in greater detail.

3.1 Experimental Procedure

In this section of the chapter, the procedure and method used for this experiment will be explain through diagram and flowchart. Figure 3.1 show the flow diagram or flow chart for each of these project step started with searching for the relevant information and end with the optimization of the simulation electrical parameter.

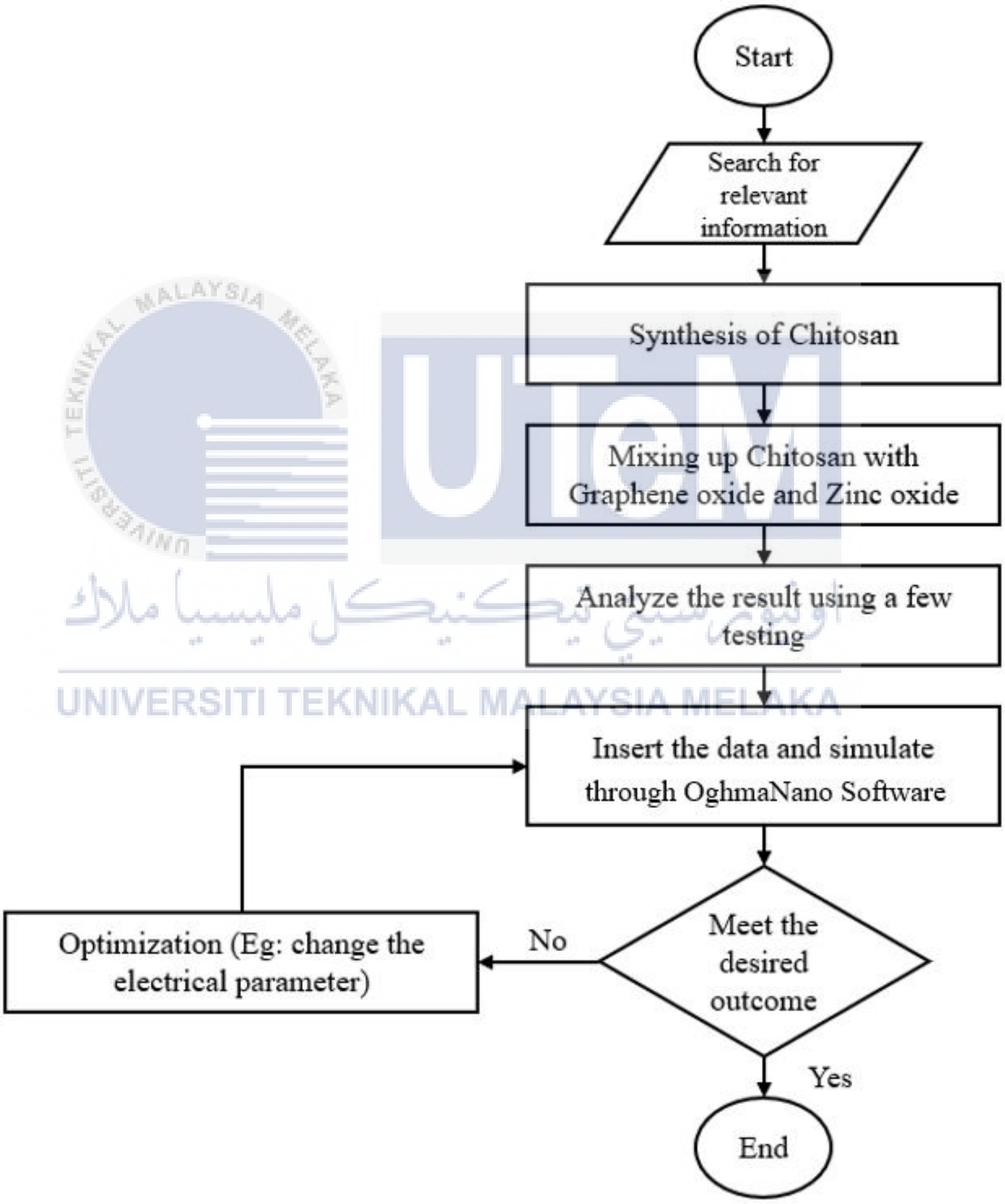

Figure 3.1: Flow chart of the experiment procedure

The procedure in this project will followed by the flowchart above which first to search and collect all the information and appropriate information depending on what this project needed through journals, books or website. Next, the synthetization of chitosan from shrimp shells will be held by using deacetylation process. Moreover, the mixture between chitosan and graphene oxide and chitosan and zinc oxide will be held after the synthetization of chitosan success. Next, all the sample will be sent to a few testing to make sure the sample turn out to be as in the journals.

Once the data is received, the following step which is simulation through OghmaNano software will be held. The data will be extracted by using Engauge Digitizer before simulated in OghmaNano. This software includes all of the physical models required to simulate inverted perovskite solar cell in both the steady state and time-domain such as the Power Conversion Efficiency (PCE), Open Circuit Voltage (Voc) and Fill Factor (FF) in the simulation.

Below shown at Figure 3.2 related to each of the following step to synthesize the chitosan from collect the shrimp shell, washed it and drying it till the process of the characterization of the mixture. Each step must be followed to make sure that all the process meet the requirement of the chitosan.

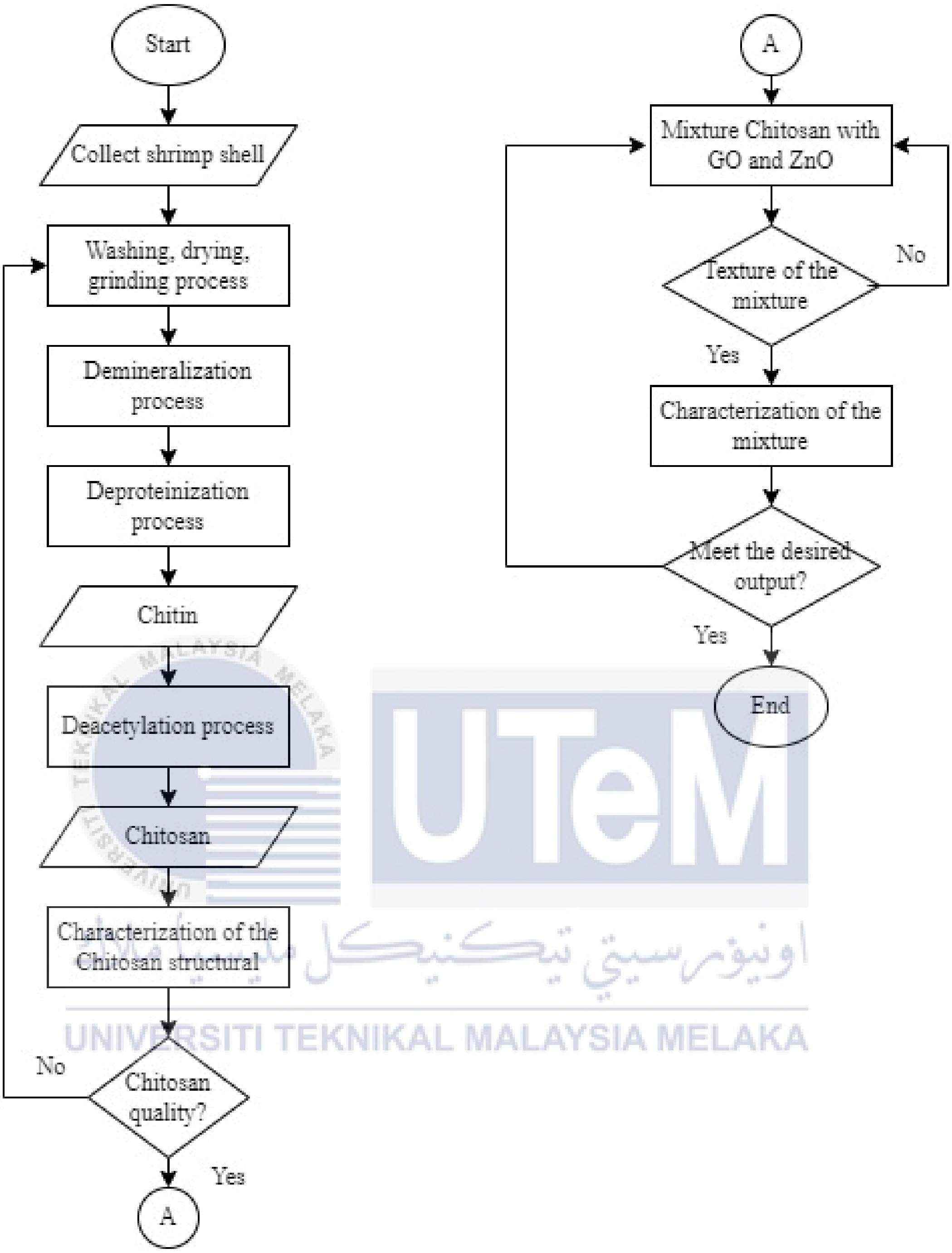

Figure 3.2: Flowchart diagram synthesis of the chitosan

3.2 Experimental Material and Equipment

The Table 3.1 and Table 3.2 below show the list of chemicals used and list of the device or equipment that will be applied in this project. All the chemicals were used without any further modification.

Table 3.1: List of Materials

No.	Materials	Formula
1.	Shrimp Shell	-
2.	Hydrochloric Acid	HCL
3.	Sodium Hydroxide	NaOH
4.	Graphene Oxide (GO)	$C_{140}H_{42}O_{20}$
5.	Zinc Oxide (ZnO)	OZn
6.	Isopropyl Alcohol (IPA)	C_3H_8O
7.	Ethanol	CH_3CH_2OH
8.	Distilled Water	H_20

Table 3.2: List of Device and Equipment Used

No.	Device and Equipment
1.	Electronic Scale
2.	Digital Multimeter
3.	Ultrasonic Bath
4.	Hotplate Stirrer
5.	Spin Coater
6.	Oven
7.	Water Distiller
8.	Filter Vacuum
9.	Fourier-Transform Infrared Spectroscopy (FTIR)
10.	Ultraviolet-Visible Spectroscopy (UV-Vis)
11.	Particle Size Analyzer (PSA)
12.	X-Ray Diffraction (XRD)
13.	Scanning Electron Microscope (SEM)

3.3 Sample Preparation

There are several techniques to get the chitosan. Deacetylation process is selected for synthetization. The student will explain each of the process of deacetylation for shrimp shell in this section. Each of the step experimental will be showed below.

3.3.1 Cleaning the glass

The Figure 3.3 below shows the step of cleaning ITO glass. Firstly, by using glass cutter tool, cut the glass into the size 1.5cm x 2cm. After cutting the glass, put the glass into a beaker and washed it using soap for 5 times. Then, immersed the glass with ethanol and put it in ultrasonic bath for 30 minutes. After that, remove the leftover ethanol and immersed it back with isopropyl alcohol. Put it in ultrasonic for another 30 minutes. Removed the leftover IPA and rinsed the glass by using distilled water. Dry the glass in oven for 15 minutes at 100˚

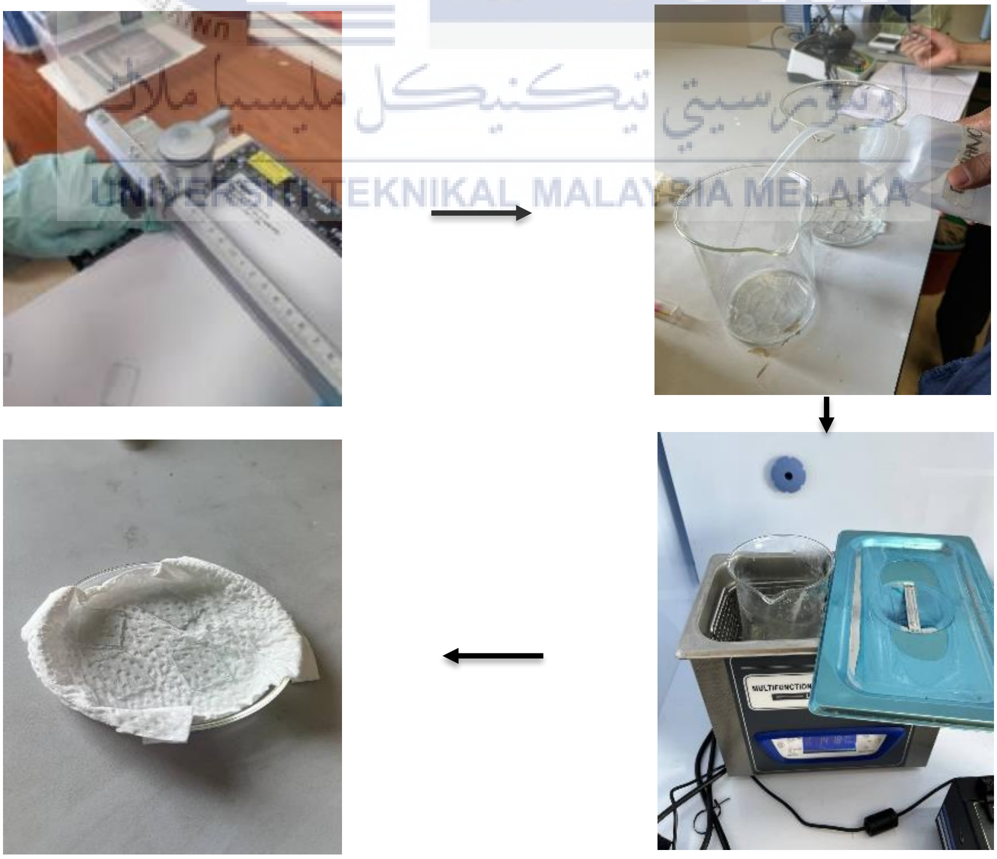

Figure 3.3: The process of cleaning ITO glass

3.3.2 Synthesis of Chitosan

Synthesis of chitosan will involve three following process which is demineralization, deproteinization and deacetylation process which it will started by preparing the shrimp shell.

3.3.2.1 Preparation of Shrimp Shell

Collect the shrimp shell. The abandoned shrimp shell is washed thoroughly by using tap water to remove all the impurities. Then, dried the shrimp shell in the oven at 90˚ for 12 hours. Once the shrimp shell being dried, crushed the dried shrimp shell with a blender till it finely crushed and finally stored it in room temperature. Figure 3.4 shows the process from washing the shrimp shell till blended it fine well.

Figure 3.4: The process of grinding the dried shrimp shell

3.3.2.2 Demineralization Process

Demineralization process is a process where to remove the mineral salts from the dried shrimp shell by using ions exchange. It also used to remove the mineral contaminant from the ionic mineral.

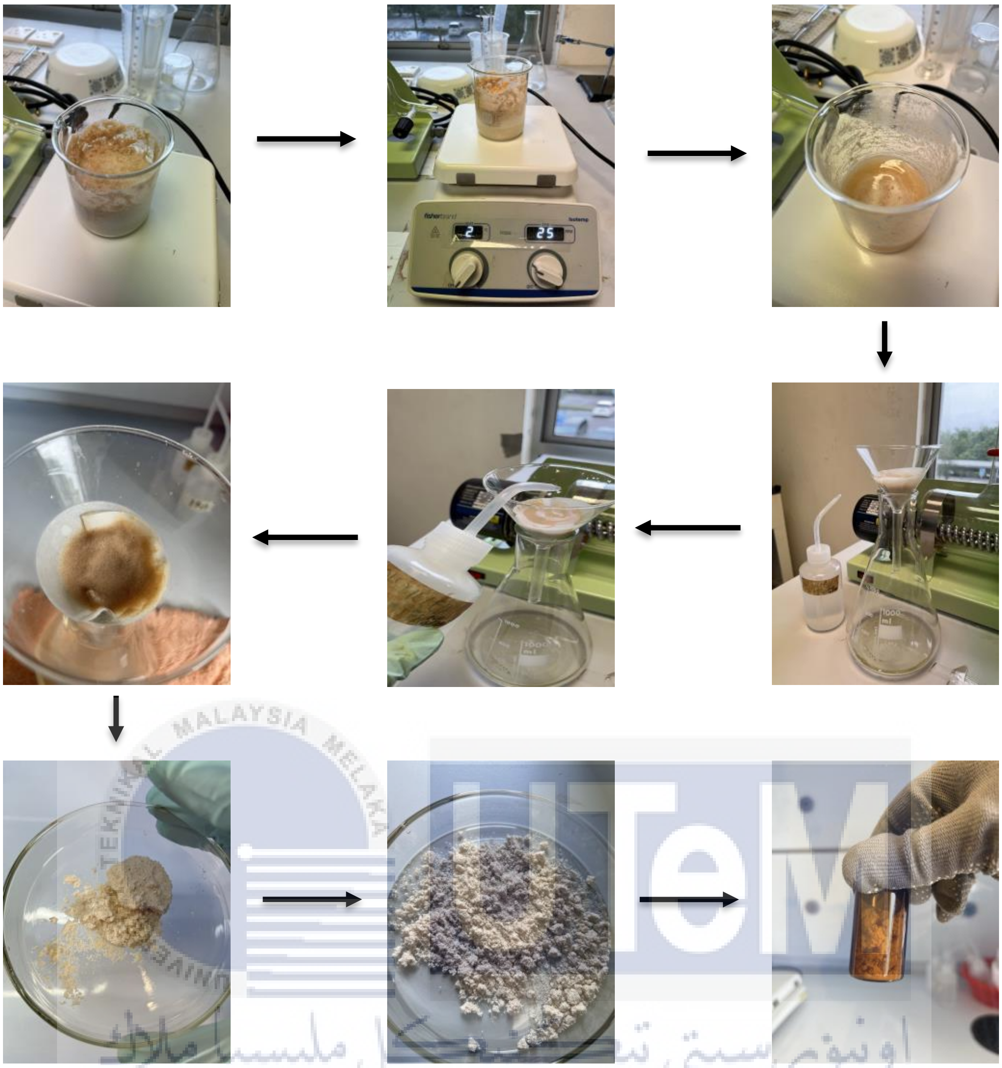

Figure 3.5: The process of demineralization

Figure 3.5 above shows the process of demineralization process. Started with weigh the dried shrimp shell for 10g and put it in a beaker of 500mL. Measure 100mL of hydrochloric acid (HCL) and poured it in the beaker slowly. Add the magnetic bar and placed the beaker on the magnetic stirrer. Agitating the mixture at 250rpm for 2 hours at room temperature.

After finish stirred, filtrated the mixture by using filter paper. Washed the mixture using distilled water until it reaches neutral pH which is pH7. Wait till it fully dried.

Put the dried shrimp shell into a beaker and immersed it in ethanol for 10 minutes for bleaching purpose then filtered.

After it fully dried, place the sample into a glass petri dish and set the oven at 70˚ for 4 hours. Put the petri dish in the oven and wait for the sample to dried. Keep the sample into a small container and it can be used for the next process which is deproteinization process.

3.3.2.3 Deproteinization Process

As for preparation of 1M NaOH, 40g of sodium hydroxide pallet with 1000mL distilled water is needed. For 100mL of 1M NaOH solution, 4g of sodium hydroxide pallet and 100mL of distilled water is needed. First, weigh the sodium hydroxide pallet by using electronic scale to 4g, and by using cylinder, measure 100mL of distilled water. Mixed it together in a beaker and put magnetic bar inside it. Stir on the magnetic stirrer with 250rpm at room temperature. Stir it around 30 minutes until the pallet is fully dissolved. Cover the beaker with parafilm to avoid other foreign matter inside it. Figure 3.6 below show the process to prepare the solution of NaOH solution.

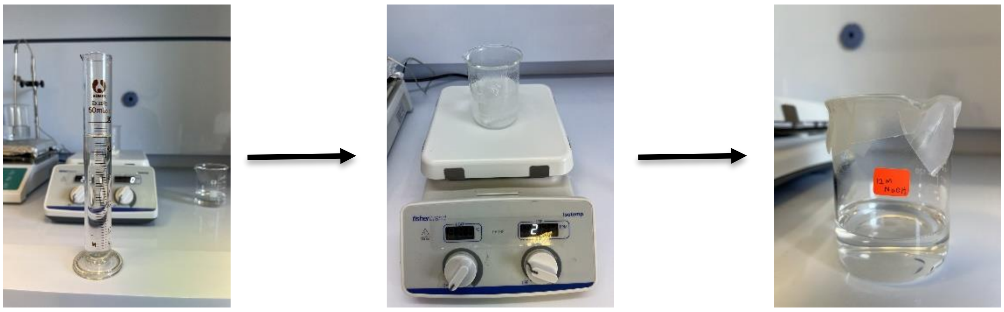

Figure 3.6: The preparation of 1M NaOH solution

Deproteinization is a process where the protein is being removed from the sample. This process of removing the protein can be done either by precipitation of the protein from a solution or by doing hydrolysis of protein with proteolytic enzymes. Figure 3.7 below show each of the deproteinization process.

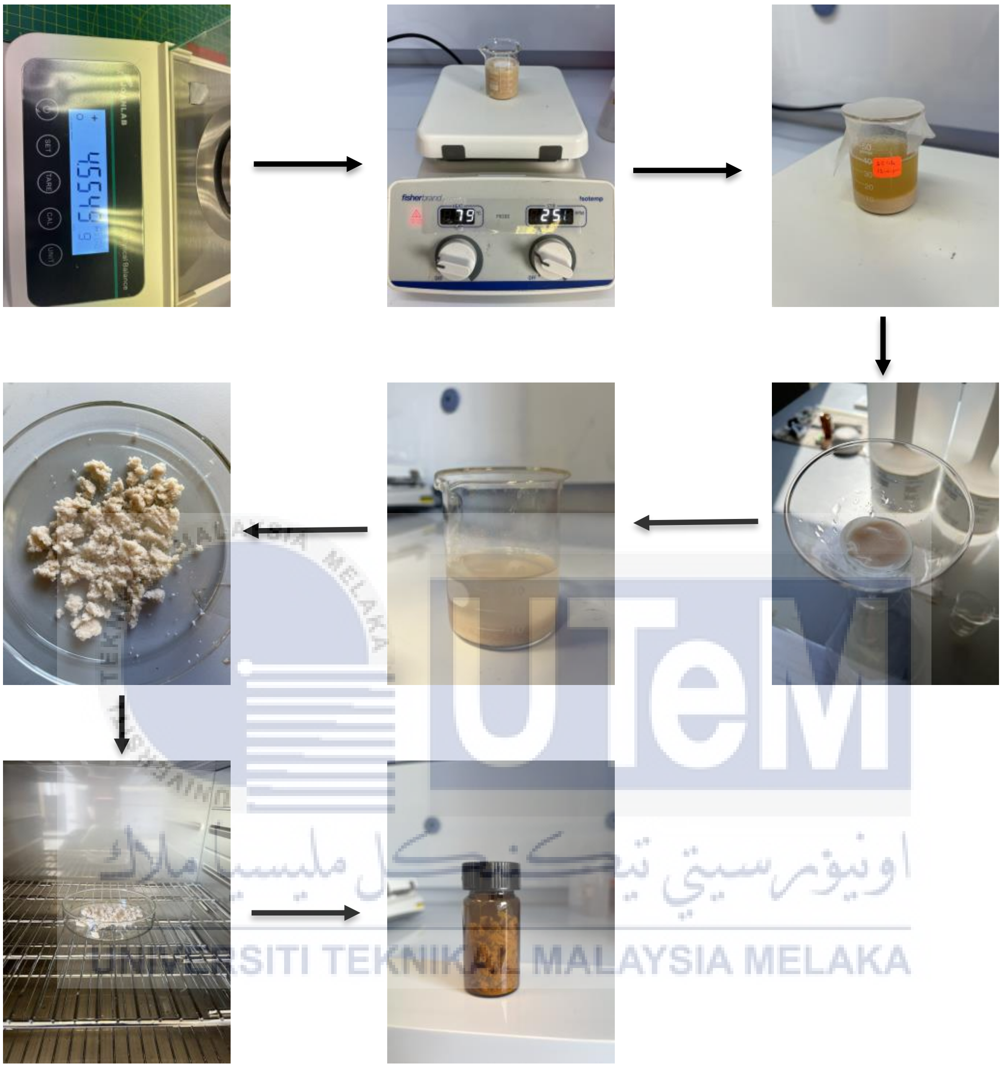

Figure 3.7: The process of deproteinization

To proceed this deproteinization process, weigh the dried shrimp shell after the demineralization process. Prepare the 1M NaOH solution. The dried shrimp shell is poured into the beaker and slowly added the NaOH solution by ratio of 1:10 (solid/liquid). Put the magnetic bar and placed the beaker on the stirrer. Set the magnetic stirrer to 250rpm at 80˚ for 2 hours.

Once it finished stirred, let it soaked for 1 day. After 1 day, filtrated the mixture by using filter paper. Washed the mixture using distilled water until it reaches neutral pH which is pH7. Wait till it fully dried. Put the dried shrimp shell into a beaker and immersed it in ethanol for 10 minutes for bleaching purpose then filtered.

After it fully dried, place the sample into a glass petri dish and set the oven at 70° for 4 hours. Put the petri dish in the oven and wait for the sample to dried. Keep the sample into a small container and it can be used for the next process which is deacetylation process. From this deproteinization process, chitin has been produced.

3.3.2.4 Deacetylation Process

As for preparation of 12.5M NaOH, 500g of sodium hydroxide pallet with 1000mL distilled water is needed. For 100mL of 12.5M NaOH solution, 50g of sodium hydroxide pallet and 100mL of distilled water is needed. First, weigh the sodium hydroxide pallet by using electronic scale to 50g, and by using cylinder, measure 100mL of distilled water. Mixed it together in a beaker and put magnetic bar inside it. Stir on the magnetic stirrer with 250rpm at room temperature. Stir it around 1 hour until the pallet is fully dissolved. Cover the beaker with parafilm to avoid other foreign from entering the beaker. Figure 3.8 below show the preparation of 12.5M of NaOH solution.

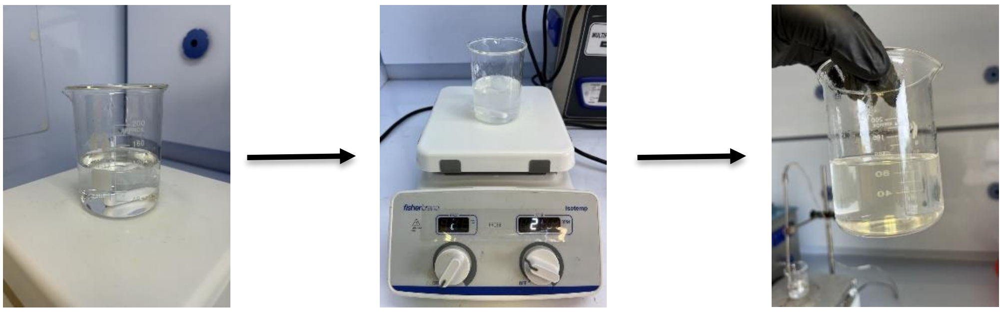

Figure 3.8: The preparation of 12.5M NaOH solution

Deacetylation is a process where chitin is used with strong NaOH solution for a hydrolysis of acetamide. The strong NaOH solution is used to produce the amino group of a new compounds which is chitosan. Figure 3.9 shown that each of the process from chitin mixed well with 12.5M NaOH solution to form chitosan.

Figure 3.9: The process of deacetylation

To get the chitosan, deacetylation process is a must. Firstly, weigh the chitin and prepare the 12.5M NaOH solution. Put the chitin into the beaker and slowly added the NaOH solution by ratio of 1:15 (solid/liquid). Put the magnetic bar and placed the beaker on the stirrer. Set the magnetic stirrer to 250rpm at 80˚ for 2 hours.

Once it finished stirred, let it soaked for 1 day. After 1 day, filtrated the mixture by using filter paper. Washed the mixture using distilled water until it reaches neutral pH which is pH7. Wait till it fully dried. Put the dried shrimp shell into a beaker and immersed it in ethanol for 10 minutes for bleaching purpose then filtered.

After it fully dried, place the sample into a glass petri dish and set the oven at 70˚ for 4 hours. Put the petri dish in the oven and wait for the sample to dried. By doing this, chitosan is formed in white type of powder. Keep the chitosan into a small container and place it into silica gel to remain the dryness of the chitosan.

3.3.3 Chitosan Aqueous

To prepare the chitosan aqueous, weigh the chitosan powder for 0.2g. Measure the 0.1% (v/v) acetic acid solution by the ratio of 1:100 (solid/liquid). As for 0.2g of chitosan powder, 20mL of acetic acid is needed. Mixed the powder and the acetic acid and put the magnetic bar. Place the mixture on top of the magnetic stirrer and set the magnetic stirrer at 30˚ with 250rpm for 1 hour and 30 minutes. Prepare 1M of NaOH solution and slowly drop into the solution. Measure the pH value of the aqueous while dropping the NaOH solution until it neutralized the aqueous at pH7. Stir for another 30 minutes. Keep the solution at room temperature and cover it using parafilm. The chitosan aqueous is ready to use. Figure 3.10 shown the process to form the chitosan aqueous.

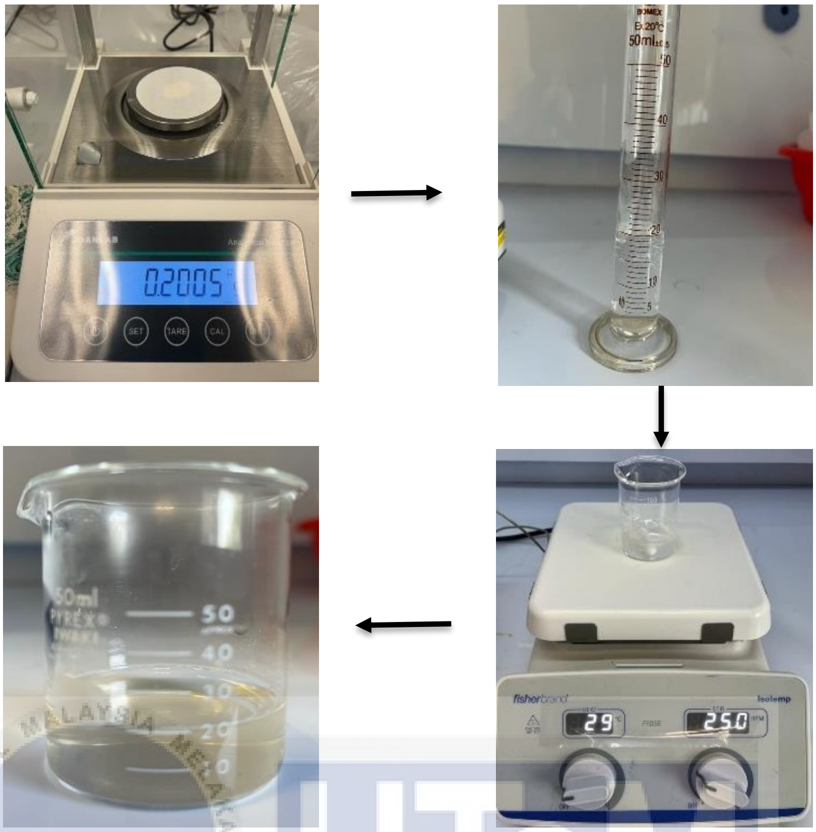

Figure 3.10: The chitosan aqueous process

3.3.4 Chitosan – Graphene Oxide

The electronic pH meter must be calibrated first before used it. First, prepare the buffer solutions of pH7, pH4 and pH10. Washed the tip of the pH electrode with distilled water and dried the tip using a tissue before dip it in the buffer solutions. Put the pH electrode into pH7 buffer solutions then washed it using distilled water and dried it back. Proceed with pH4 and lastly pH10. Check the slope efficiency and the slope efficiency must be more than 92% to get the accurate calibration of the pH value. pH value calibrator must be check step-by-step as shown at Figure 3.11 to get the accurate pH value while having the best result of the output.

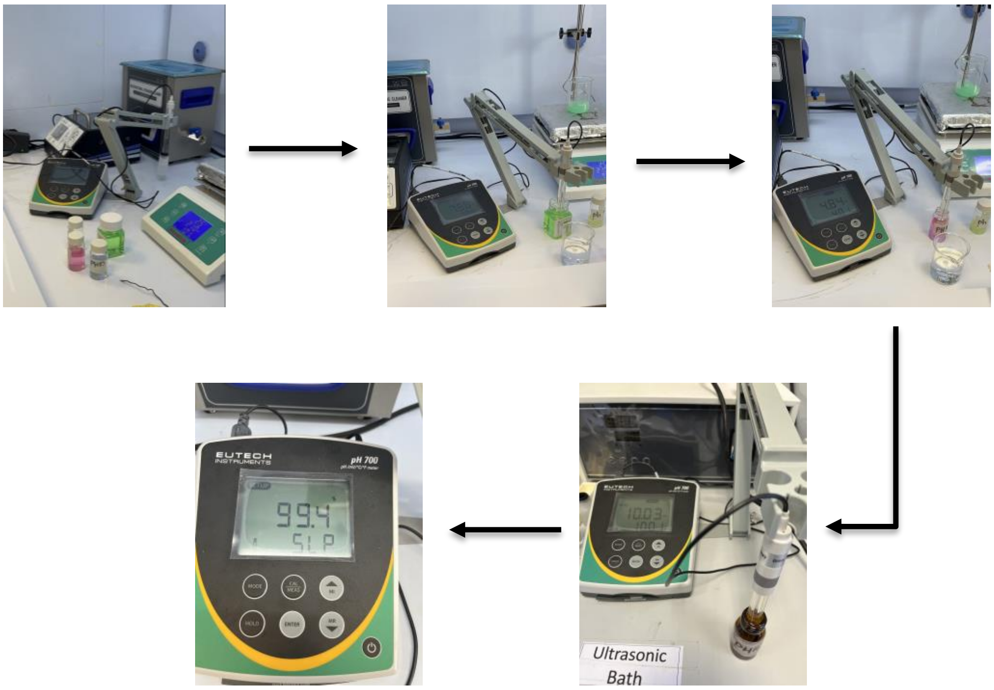

Figure 3.11: The process to calibrate the electronic pH meter

Firstly, weigh the chitosan powder for 0.1g and dissolved the chitosan powder in 1wt% of aqueous acetic acid with ratio of 1:100 (solid/liquid) to form chitosan solution. Put the magnetic bar and turn on the magnetic stirrer with 250rpm at room temperature for 1 hour.

Prepare the graphene oxide by dissolved it in 20mL of distilled water and then treated with ultrasonic bath for 45 minutes. Mixed the graphene oxide into the chitosan solution and continue stir for another 1 hour. Check the pH of this mixture by dipping the pH electrode into the solution. Prepare 1M of NaOH solution and slowly drop into the solution. Slowly drop the NaOH solution till the pH meter showed value 6pH which is neutral pH. Continue stir for another 4 hours and keep the solution at room temperature. Sonicate the solution whenever to use it. Chitosan-graphene oxide solution is prepared. Figure 3.12 shown the process to mixed chitosan and the graphene oxide.

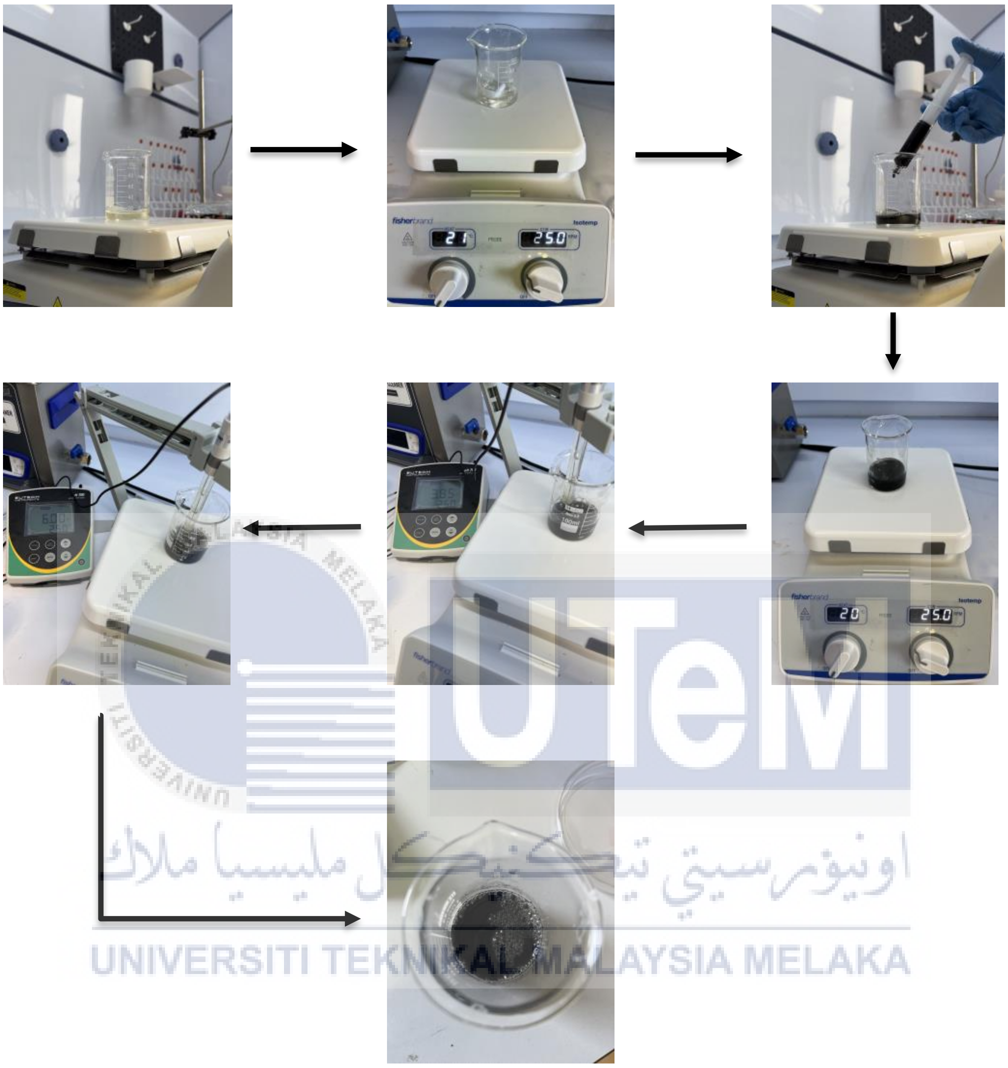

Figure 3.12: The process of mixture between Chitosan and Graphene Oxide

3.3.5 Chitosan – Zinc Oxide

Weigh the chitosan powder for 0.1g and dissolved the chitosan powder in 1wt% of aqueous acetic acid with ratio of 1:100 (solid/liquid) to form chitosan solution. Put the magnetic bar and turn on the magnetic stirrer with 250rpm at room temperature for 1 hour.

Weigh 0.1g of zinc oxide pallet and dissolve it in the chitosan solution. Continue stir for another 1 hour. Check the pH of this mixture by dipping the pH electrode into the solution. Prepare 1M of NaOH solution and slowly drop into the solution. Slowly drop the NaOH solution till the pH meter showed value 6pH which is neutral pH. Continue stir for another 4 hours and keep the solution at room temperature. Figure 3.13 below shown the chitosan-zinc oxide solution is prepared.

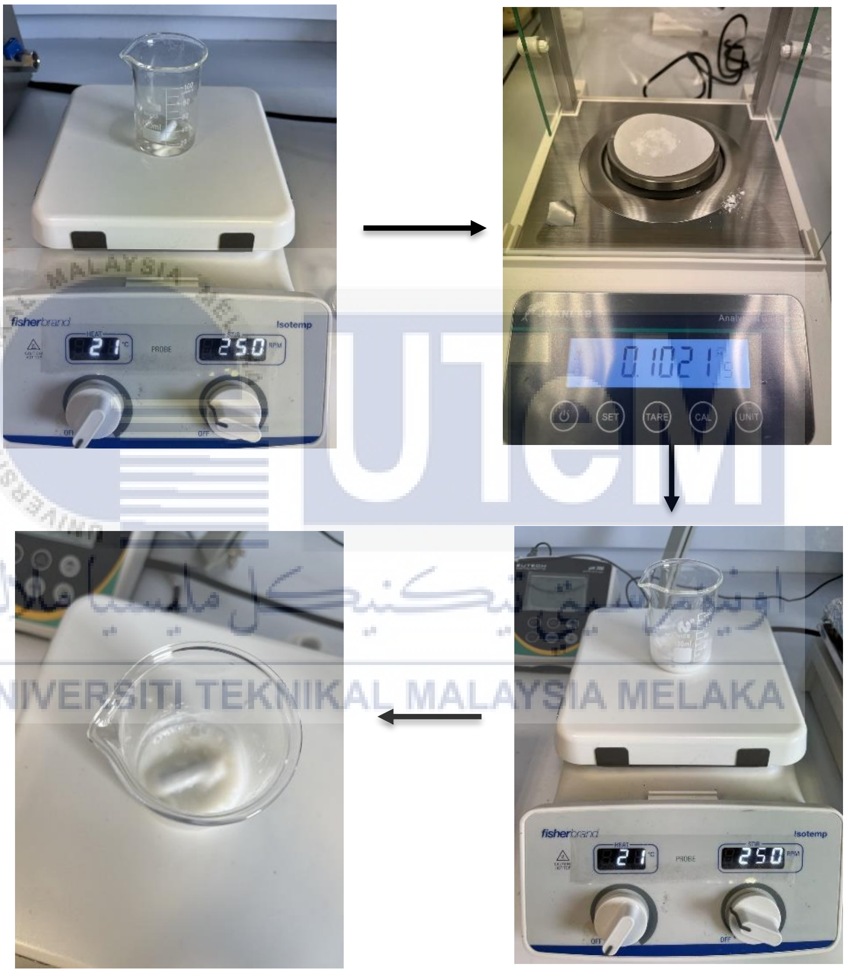

Figure 3.13: The process of mixture between Chitosan and Zinc Oxide

3.4 Simulation of Perovskite Solar Cell

This simulation proses will start with extracting the data from absorption index and refractive index by using Engauge Digitizer and the data will be export into the OghmaNano software. Each of these process will be shown below.

3.4.1 Adding New Material in Engauge Database

1. New material can be added if the materials is not listed in OghmaNano database such as MaPbI$_3$. The first step is to get the refractive index, a and absorption index, n from the previous research paper, journal or books. Figure 3.14 shows the example of absorbance index and refractive index for MaPbI3.

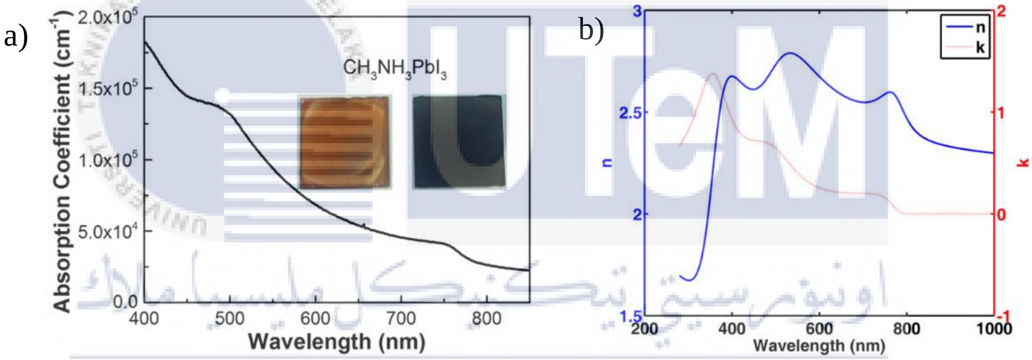

Figure 3.14: (a) Absorbance index for MaPbI3, (b) Refractive index for MaPbI3

2. Next, download and install the Engauge Digitizer software from the website https://www.softpedia.com/get/Science-CAD/Engauge-Digitizer.shtml#download.

DOWNLOAD Engauge Digitizer 12.1 for Windows

Figure 3.15: Engauge Digitizer download software

3. Once the installation is done, import the image of refractive and absorption that containing the graph. Select the point by point along the curve of the graph. Figure 3.16 show how to plot the blue tick along the curve of the graph.

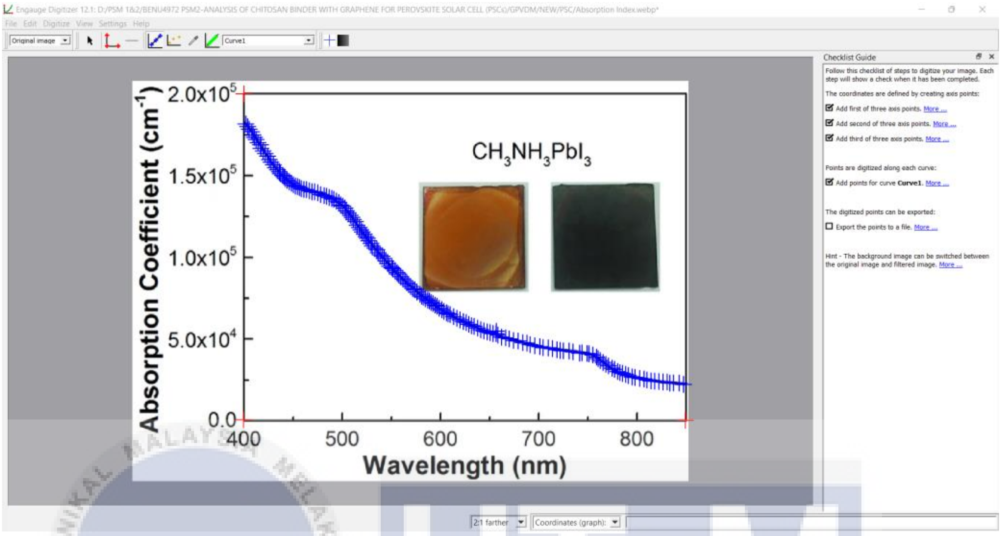

Follow this checklist of steps to digitize your image. Each step will show a check when it has been completed.

The coordinates are defined by creating axis points:

☑ Add first of three axis points. More ...
☑ Add second of three axis points. More ...
☑ Add third of three axis points. More ...

Points are digitized along each curve:

☑ Add points for curve **Curve1**. More ...

The digitized points can be exported:

☐ Export the points to a file. More ...

Hint - The background image can be switched between the original image and filtered image. More ...

Figure 3.16:Tick on the points along the curve of the graph

4. Export the data from Engauge Digitizer to .csv type and save. Extract the data from excel type format to text file format. Save the text file format.
5. Repeat the same process for the other refractive index. On Figure 3.17 shown the data will be looked like on the Engauge digitizer software.

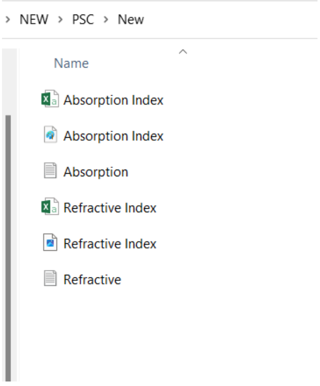
› NEW › PSC › New

Name
Absorption Index
Absorption Index
Absorption
Refractive Index
Refractive Index
Refractive

Figure 3.17: All data collected

6. The new material now can be added into the OghmaNano software.

3.4.2 Simulation in OghmaNano Software

1. Install the OghmaNano software from the website given https://www.oghma-nano.com/. Figure 3.18 shown that the window of OghmaNano website.

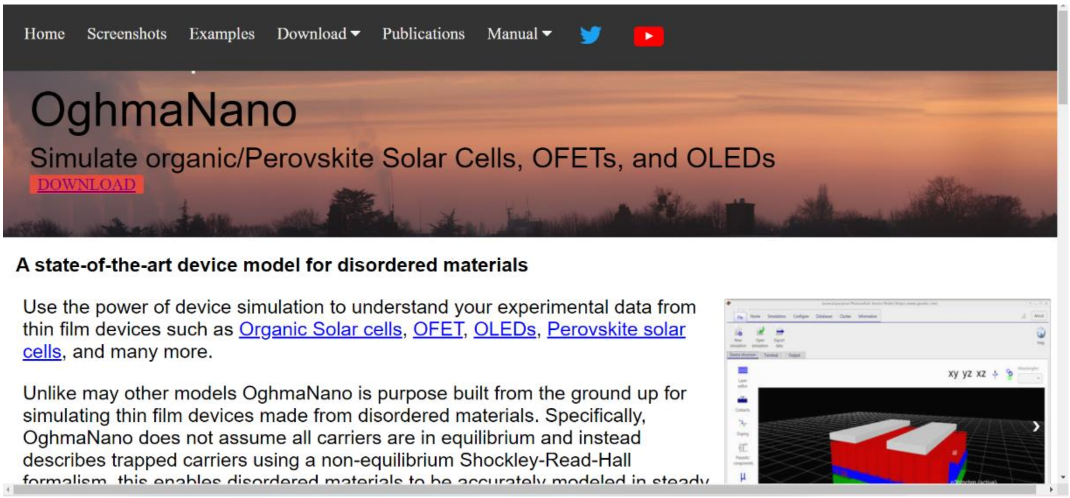

OghmaNano

Simulate organic/Perovskite Solar Cells, OFETs, and OLEDs

A state-of-the-art device model for disordered materials

Use the power of device simulation to understand your experimental data from thin film devices such as Organic Solar cells, OFET, OLEDs, Perovskite solar cells, and many more.

Unlike may other models OghmaNano is purpose built from the ground up for simulating thin film devices made from disordered materials. Specifically, OghmaNano does not assume all carriers are in equilibrium and instead describes trapped carriers using a non-equilibrium Shockley-Read-Hall formalism, this enables disordered materials to be accurately modeled in steady

Figure 3.18: OghmaNano website

2. Open the OghmaNano software and select New Simulation. Choose Organic Solar Cell. Selection of the solar cell depending on like Figure 3.19 below shown.

Which type of device would you like to simulate? (Double click to open)

Figure 3.19: Selection of solar cell

3. as shown in Figure 3.20 below, choose the type of solar cell needed to be run such as inverted perovskite solar cell and double click on it.

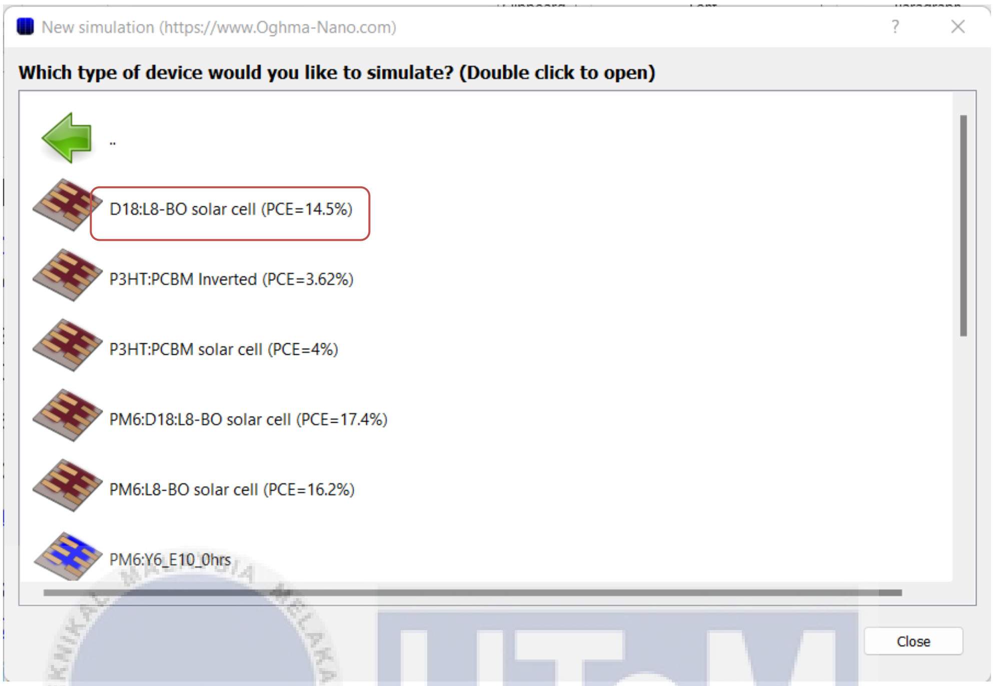

New simulation (https://www.Oghma-Nano.com)

Which type of device would you like to simulate? (Double click to open)

- ..
- D18:L8-BO solar cell (PCE=14.5%)
- P3HT:PCBM Inverted (PCE=3.62%)
- P3HT:PCBM solar cell (PCE=4%)
- PM6:D18:L8-BO solar cell (PCE=17.4%)
- PM6:L8-BO solar cell (PCE=16.2%)
- PM6:Y6_E10_0hrs

Figure 3.20: Selection type of solar cell

4. Once the window popped up, the materials and the thickness can be edit. Click Layer Editor to change the material and thickness. Figure 3.21 show the layer editor on the left of the OghmaNano window.

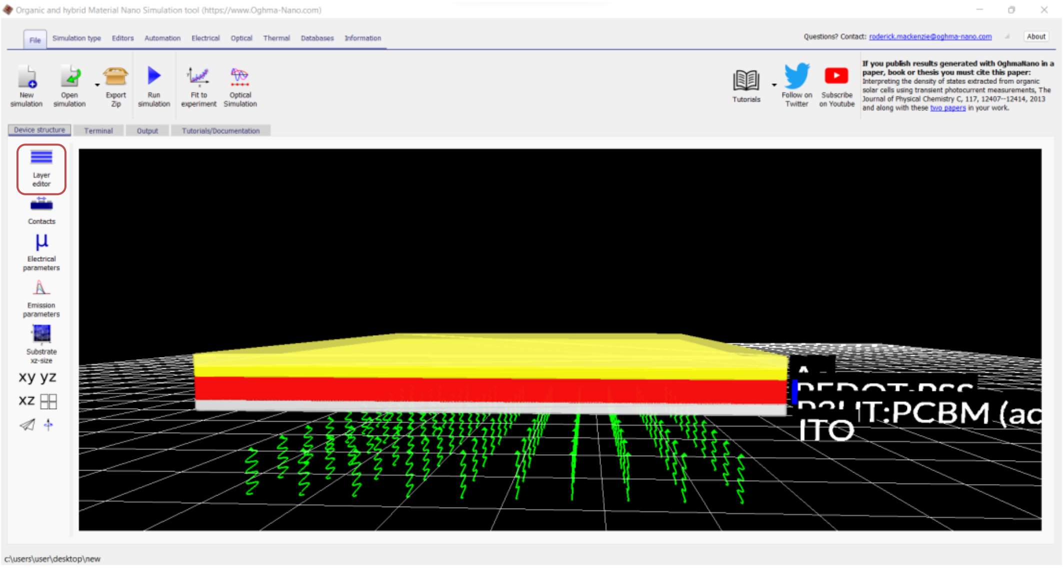

Organic and hybrid Material Nano Simulation tool (https://www.Oghma-Nano.com)

Questions? Contact: roderick.mackenzie@oghma-nano.com

If you publish results generated with OghmaNano in a paper, book or thesis you must cite this paper: Interpreting the density of states extracted from organic solar cells using transient photocurrent measurements, The Journal of Physical Chemistry C, 117, 12407--12414, 2013 and along with these two papers in your work.

c:\users\user\desktop\new

Figure 3.21: Layer Editor to change the materials and thickness

5. As shown in the figure 3.22, if the material is not given, open Database and choose Materials Database.

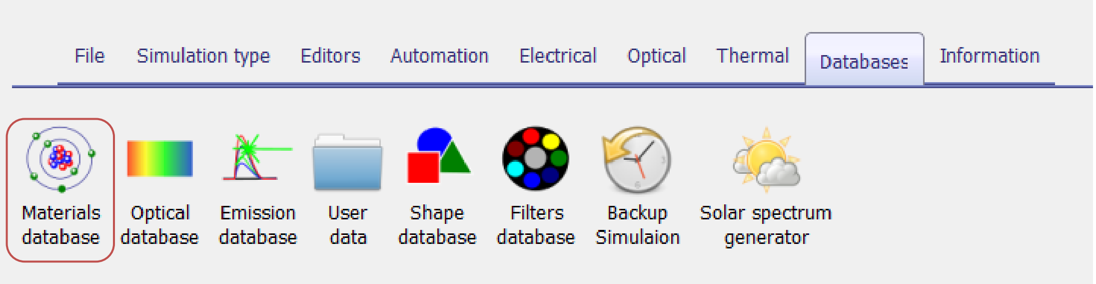

Figure 3.22: Materials Database for add new materials

6. Click Add Materials and name the new materials as shown on the figure 3.23 below.

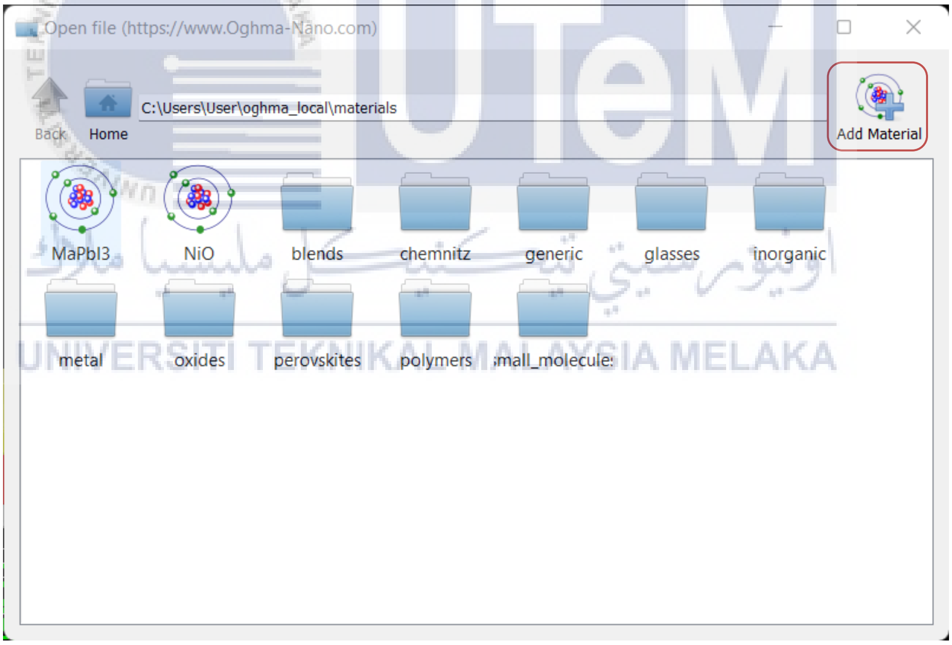
Open file (https://www.Oghma-Nano.com)

C:\Users\User\oghma_local\materials

Figure 3.23: Adding new materials

7. Click Import Data from file, and open the data that been saved in txt. type. Make sure the x-label and y-label match the data from the journal or books before.

Repeat the same method for refractive index. Figure 3.24 (a)(b) below show how the output after added new material on the OghmaNano Software.

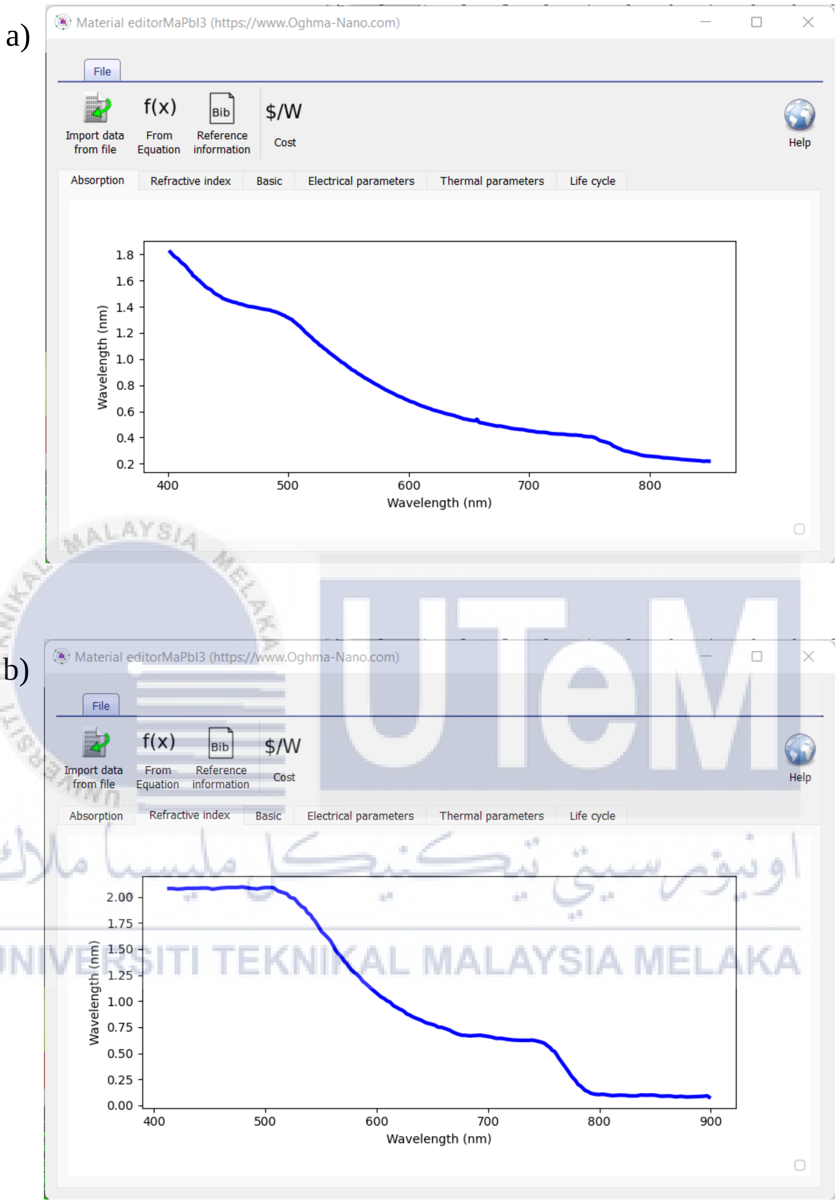

Figure 3.24: The absorption and refractive index is successfully added to the OghmaNano, (a) Absorption index, (b) Refractive index

8. The materials are ready to use. To change the simulation parameter, click Electrical Parameter to change any other parameter based on journal or books.

9. Run the simulation and open the Output command to see the result. Figure 3.25 (a) show the window popup after run the simulation, while Figure 3.25 (b) shows the simulation result on sim_info.dat.

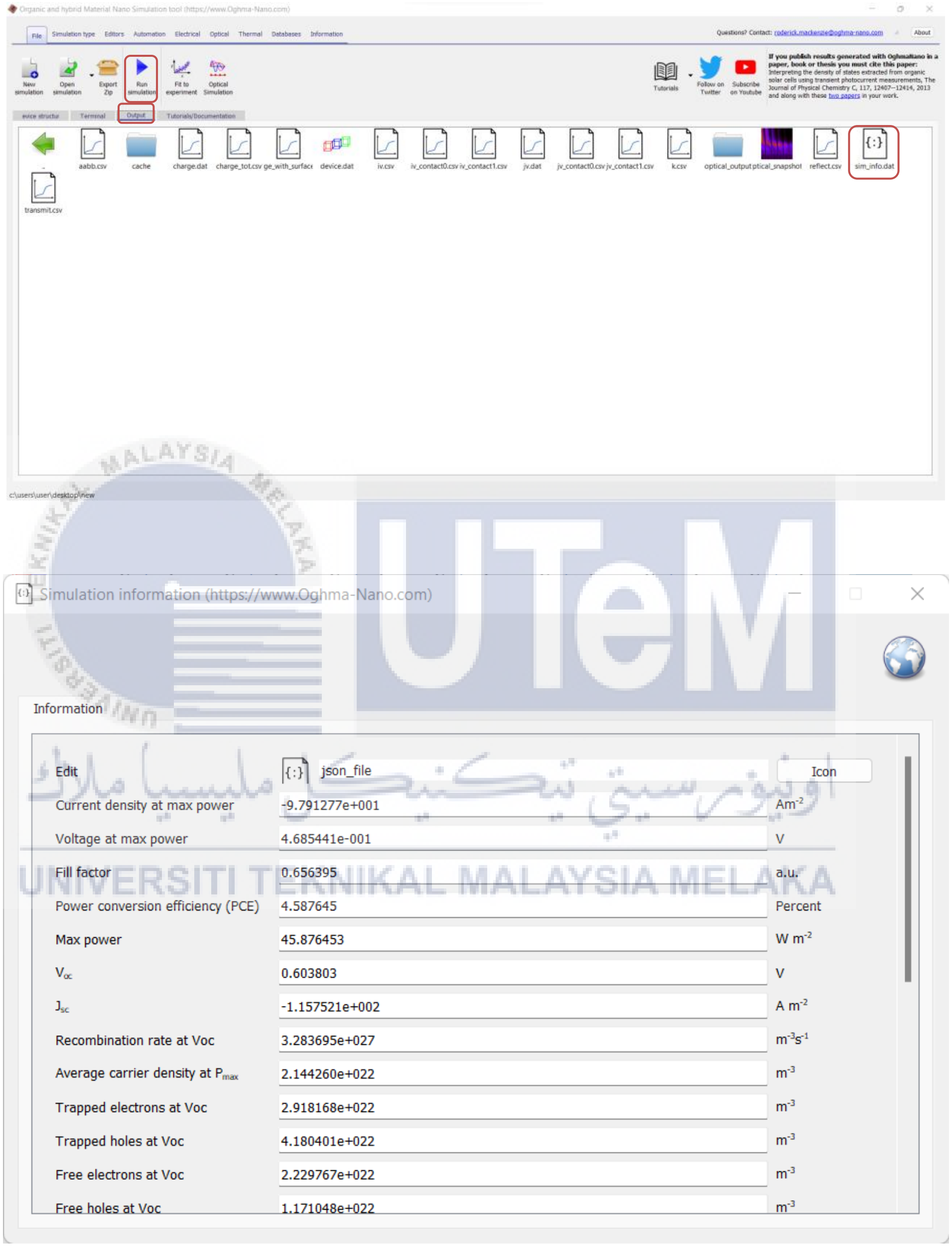

If you publish results generated with OghmaNano in a paper, book or thesis you must cite this paper: Interpreting the density of states extracted from organic solar cells using transient photocurrent measurements, The Journal of Physical Chemistry C, 117, 12407–12414, 2013 and along with these two papers in your work.

Edit	json_file	Icon
Current density at max power	-9.791277e+001	Am^{-2}
Voltage at max power	4.685441e-001	V
Fill factor	0.656395	a.u.
Power conversion efficiency (PCE)	4.587645	Percent
Max power	45.876453	W m^{-2}
V_{oc}	0.603803	V
J_{sc}	-1.157521e+002	A m^{-2}
Recombination rate at Voc	3.283695e+027	$m^{-3}s^{-1}$
Average carrier density at P_{max}	2.144260e+022	m^{-3}
Trapped electrons at Voc	2.918168e+022	m^{-3}
Trapped holes at Voc	4.180401e+022	m^{-3}
Free electrons at Voc	2.229767e+022	m^{-3}
Free holes at Voc	1.171048e+022	m^{-3}

Figure 3.25: The simulation result, (a) Output window, (b)Simulation Information

3.5 Safety Precautions

As shown on Figure 3.26, each of the student must followed all the laboratory safety equipment to make sure that there are no incident that will happen during the laboratory session.

Figure 3.26: Laboratory safety equipment

1. Always wear protective clothing including a face mask, safety glasses, chemical gloves and apron while handling the chemical.
2. Must dispose properly all the waste chemical used.
3. Avoid hands contact with face, mouth, eyes, and body while using chemical and lab equipment. Repeatedly wash hands with soap after finishing the experiment.
4. Always use appropriate laboratory equipment when handling chemicals and never use them with bare finger because all chemicals in the laboratory are considered hazardous.
5. Immediately rinse with running water for at least 20 minutes if the chemical splash in the eye.
6. Experiments should be monitored during the reaction or during heating and during observation, keep at least 1 foot away from the specimen.

CHAPTER 4

RESULTS AND DISCUSSION

The Result and Discussion chapter’s purpose is to discuss about the experiment results that have been carried. The method to achieve the experiment result has been explained in the previous chapter. The first objective of this project is to synthesize the chitosan from shrimp shell by deacetylation process. The second objective of this project is to analyze the performance, structural, electrical and optical properties of thin layer chitosan mixed with graphene and zinc oxide. The last objective is to simulate chitosan mixed with graphene and zinc oxide as Electron Transport Layer (ETL) in inverted solar cell by using OghmaNano.

4.1 Synthetization of Chitosan from Shrimp Shell by Deacetylation Process

In this subtopic, the student will discuss the result and analyzation on how to form the chitosan from scratch which is from waste shrimp shell. Each process result will be shown below.

4.1.1 Characterization of Sizing Shrimp Shell

These shrimp shell sample with time of blending will be send out to characterize and check whether there is any different in their sizing or not.

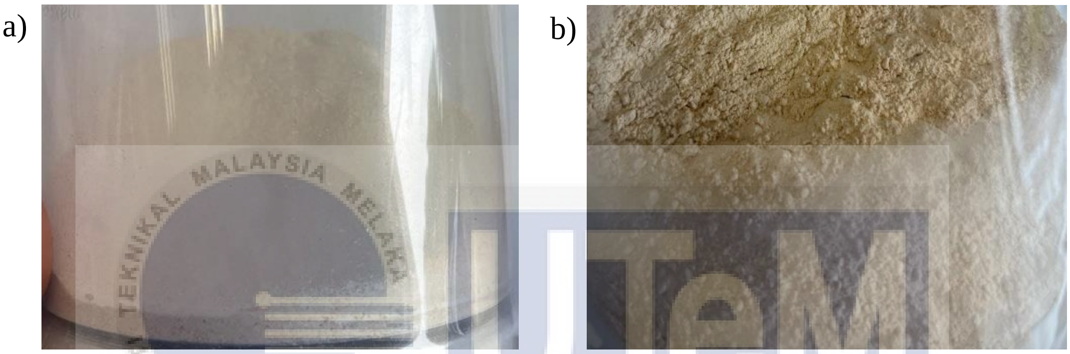

Figure 4.1: (a) Shrimp Shell sample 1, (b) Shrimp Shell sample 2

Based on the Figure 4.1 above, there are two sample of dried shrimp shell that has been grinding which has different in size. The size of shrimp shell must be the closet to the original size of the chitosan. There are two sample of dried shrimp shell that have been blended and to clarify and to confirm the size of each dried shrimp shell, particle size analysis has been done to make sure the best and the smallest particle of dried shrimp shell have been selected to proceed with the synthetization of the chitosan.

a)

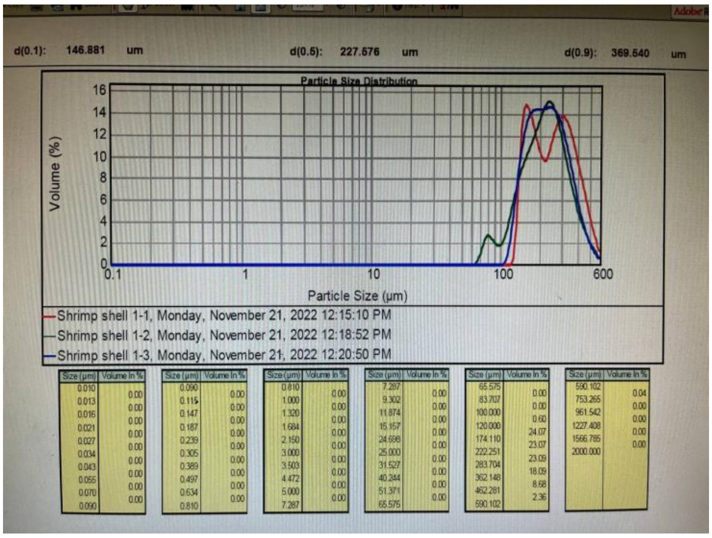

d(0.1): 146.881 um d(0.5): 227.576 um d(0.9): 369.540 um

—Shrimp shell 1-1, Monday, November 21, 2022 12:15:10 PM
—Shrimp shell 1-2, Monday, November 21, 2022 12:18:52 PM
—Shrimp shell 1-3, Monday, November 21, 2022 12:20:50 PM

Size (µm)	Volume In %	Size (µm)	Volume In %	Size (µm)	Volume In %	Size (µm)	Volume In %	Size (µm)	Volume In %	Size (µm)	Volume In %
0.010	0.00	0.090	0.00	0.810	0.00	7.287	0.00	65.575	0.00	590.102	0.04
0.013	0.00	0.115	0.00	1.000	0.00	9.302	0.00	83.707	0.00	753.265	0.00
0.016	0.00	0.147	0.00	1.320	0.00	11.874	0.00	100.000	0.60	961.542	0.00
0.021	0.00	0.187	0.00	1.684	0.00	15.157	0.00	120.000	24.07	1227.408	0.00
0.027	0.00	0.239	0.00	2.150	0.00	24.698	0.00	174.110	23.07	1566.785	0.00
0.034	0.00	0.305	0.00	3.000	0.00	25.000	0.00	222.251	23.09	2000.000	
0.043	0.00	0.389	0.00	3.503	0.00	31.527	0.00	283.704	18.09		
0.055	0.00	0.497	0.00	4.472	0.00	40.244	0.00	362.148	8.68		
0.070	0.00	0.634	0.00	5.000	0.00	51.371	0.00	462.281	2.36		
0.090		0.810		7.287		65.575		590.102			

Figure 4.2: Shrimp Shell sample 1-Particle Size Analysis

b)

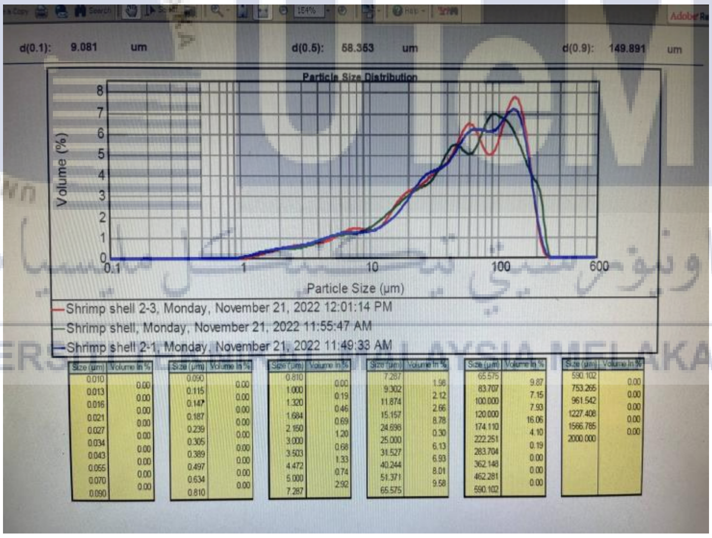

d(0.1): 9.081 um d(0.5): 58.353 um d(0.9): 149.891 um

—Shrimp shell 2-3, Monday, November 21, 2022 12:01:14 PM
—Shrimp shell, Monday, November 21, 2022 11:55:47 AM
—Shrimp shell 2-1, Monday, November 21, 2022 11:49:33 AM

Size (µm)	Volume In %	Size (µm)	Volume In %	Size (µm)	Volume In %	Size (µm)	Volume In %	Size (µm)	Volume In %	Size (µm)	Volume In %
0.010	0.00	0.090	0.00	0.810	0.00	7.287	1.98	65.575	9.87	590.102	0.00
0.013	0.00	0.115	0.00	1.000	0.19	9.302	2.12	83.707	7.15	753.265	0.00
0.016	0.00	0.147	0.00	1.320	0.46	11.874	2.66	100.000	7.93	961.542	0.00
0.021	0.00	0.187	0.00	1.684	0.69	15.157	8.78	120.000	16.06	1227.408	0.00
0.027	0.00	0.239	0.00	2.150	1.20	24.698	0.30	174.110	4.10	1566.785	0.00
0.034	0.00	0.305	0.00	3.000	0.68	25.000	6.13	222.251	0.19	2000.000	
0.043	0.00	0.389	0.00	3.503	1.33	31.527	6.93	283.704	0.00		
0.055	0.00	0.497	0.00	4.472	0.74	40.244	8.01	362.148	0.00		
0.070	0.00	0.634	0.00	5.000	2.92	51.371	9.58	462.281	0.00		
0.090		0.810		7.287		65.575		590.102			

Figure 4.3: Shrimp Shell sample 2-Particle Size Analysis

Based on the Figure 4.3 (a)(b) above, the first shrimp shell (a) is having sizing at the range of 100-600µm and the second dried shrimp shell (b) is in the range of 1-200µm. To proceed with the synthetization of chitosan, the smallest particle must be selected and with the specific range given, the shrimp shell 2 is better and have smallest particle than the shrimp shell 1 because the range of the size is smallest up to 1μm. The smallest the particle, the best output result it will be and it will be easier to dissolve during the process.

4.1.2 Synthetization of the Chitosan

Synthetization of the chitosan was done by using the deacetylation process. Through this process, several samples have been made to obtain differences output. The parameter has been made based on the difference in time and temperature. Table 4.1 below show, 3 samples parameters that have been taken that are differentiated by temperature and execution time.

Table 4.1: The differences parameter based on temperature and time

Sample/Process	**Demineralization**		**Deproteinization**		**Deacetylation**	
	Time, h	Temp.˚c	Time, h	Temp.˚c	Time, h	Temp.˚c
Sample 1	2	21	2	80	2	80
Sample 2	2	**70**	2	**80**	2	**90**
Sample 3	**4**	21	**4**	80	**4**	80

Each of the sample have the same time taken on the drying in the oven for each of this process which is for 4 hours. This difference is all done during the stirrer process on the magnetic plate. These two parameters are considered because to ensure that each process has a difference in the end result which is chitosan. As for Sample 1, the time taken and the temperature is referred based on the journal[21]. Sample 2 is being differentiate by changing the temperature while stirring and keep maintain the time taken. As for Sample 3, the temperature is kept maintain while the time to stir the sample on the magnetic stirrer was changed. Below shows the output of the chitosan for sample 1, sample 2 and sample 3.

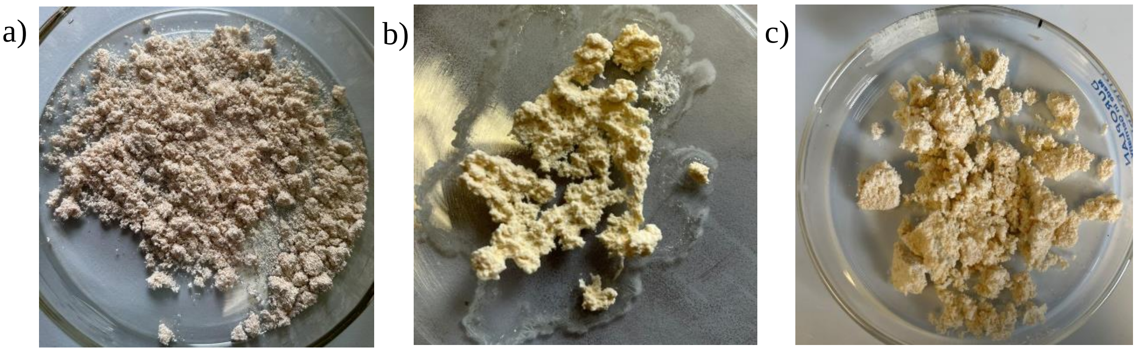

Figure 4.4: (a) Chitosan Sample 1, (b) Chitosan Sample 2, (c) Chitosan Sample 3

Refer to figure 4.4, (a), (b), (c) is the result after completing deacetylation process. Sample 1 and Sample 3 become white and powdery, while for sample 2, it turns to white and a bit of flaky. This may be affected by the changing temperature during the entire process. This 3 sample have been sent to have Fourier Transform Infrared Spectroscopy (FTIR) to quickly and definitively identify the compounds of the sample.

4.2 Analyze the performance, structural, electrical and optical properties of thin layer Chitosan mixed with Graphene and Zinc Oxide.

In this subtopic, the student will discuss about the structural, the performance electrical conductivity and the optical properties of the chitosan after passing through the process of deacetylation process. Each process result will be shown below.

4.2.1 Degree of Deacetylation (DA)

The degree of deacetylation (DA) was determined in triplicate by Fourier Transform Infrared Spectroscopy (FTIR) and recorded at room temperature from 4000nm. to 400nm. DA was calculated from the spectra using Equation (1):

$$DA(\%) = \left(\frac{A_{1655}}{A_{3450}}\right) x \frac{100}{1.33} \qquad (1)$$

Refer to this equation, A_{1655} and A_{3450} represent the absorption index of chitosan at 1655nm. and 3450nm. respectively. There are 4 sample that have been send for FTIR spectroscopy which include chitosan purchased from (Chemiz.my). Chitosan from Chemiz.my is included because of to get a mark point between the sample made by the deacetylation process and purchased one. Table 4.2 shows the comparison of the transmittance index between each sample.

Table 4.2 : Comparison of transmittance index value between samples

Sample	1655nm.	3450nm.
Chemiz.my	81.99	86.24
Sample 1	87.04	90.63
Sample 2	74.65	79.50
Sample 3	90.88	96.15

The Degree of deacetylation (DA) shows the percentage of chitosan that have been turned from chitin. It is important to know as it indicates the quality of chitosan. Equation (1) was used to calculate DA from the FTIR spectrum. Table 4.3 below shows the calculated degree of deacetylation value of the synthesis chitosan.

Table 4.3: Degree of Deacetylation for every sample of Chitosan

Sample	Degree of Deacetylation (%)
Chemiz.my	71%
Sample 1	72%
Sample 2	70%
Sample 3	71%

Table 4.3 show that the sample of chitosan from Chemiz.my obtains a 71% of degree of deacetylation, which is classified in the middle degree of deacetylation.

Sample 1, sample 2, and sample 3 obtain middle degree of deacetylation of 72%, 70% and 71% respectively. Sample 1 have achieved the highest number degree of deacetylation of 72% compared to the other samples. This can be concluded that, sample 1 as the best synthetization of chitosan to be used for the solar cell fabrication.

4.2.2 Fourier Transform Infrared Spectroscopy

Fourier Transform Infrared technique (FTIR) was developed to determine all organic components, including chemical bonds and organic content, simultaneously. Figure 4.5 below show the FTIR spectra of the chitosan samples.

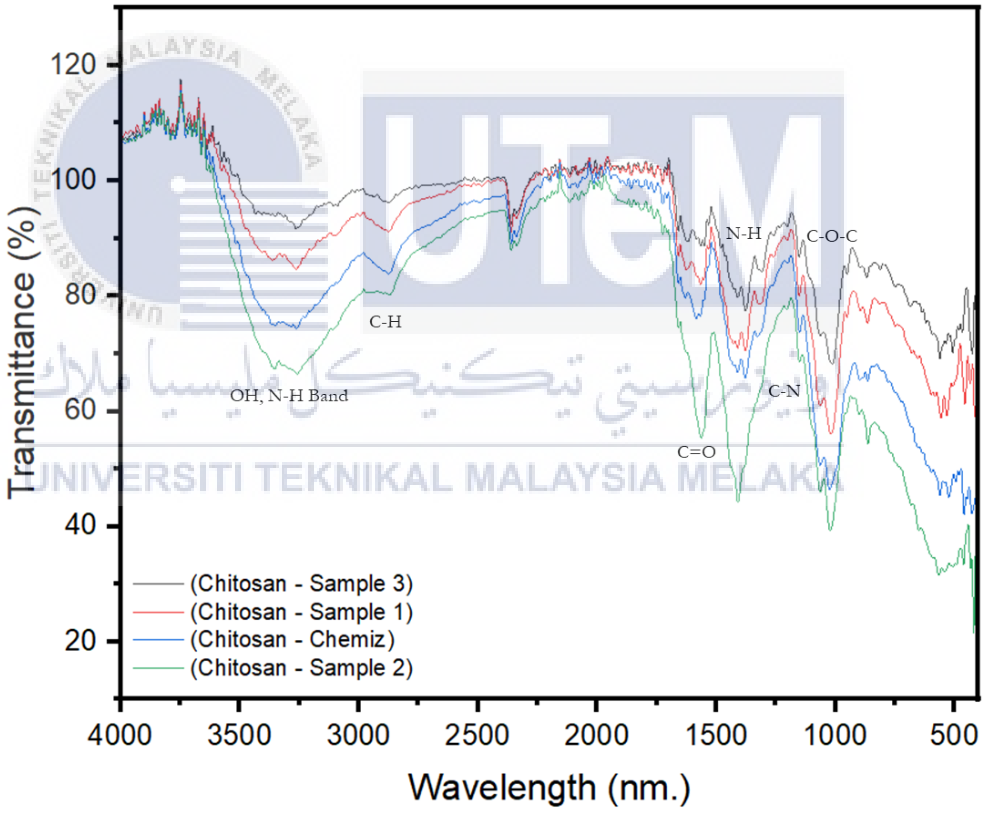

Figure 4.5: FTIR Spectra of Chitosan Sample

Refer to the figure 4.5 above shows that the relative peaks for chitosan can be seen in the FTIR spectrum. A strong and broad extending O-H peak with N-H peak at peak 3349nm. Next, C-H is depicted at 2873nm. at peak axial expansion. The C=O stretch (amide I), N-H bending (amide II), and C-N stretching (amide III) corresponded to the three type of chitosan groups, which are described with 1565nm. 1517nm and 1407nm. respectively. The peaks of C-O-C drop at the peak of 1020nm. which is the extended oscillation of the skeleton. Sample chemiz.my, sample 1, sample 2, and sample 3 spectrum can be seen to be almost identical with a bit of differences at certain reflectance.

4.2.3 UV-Vis Spectrum

UV-Vis is a technique for quantifying organic substances and inorganic metals based on their absorbance or reflectance at certain light wavelengths. Since chitosan from sample 1 has the highest number degree of deacetylation, it will be use to mixture with graphene oxide and zinc oxide.

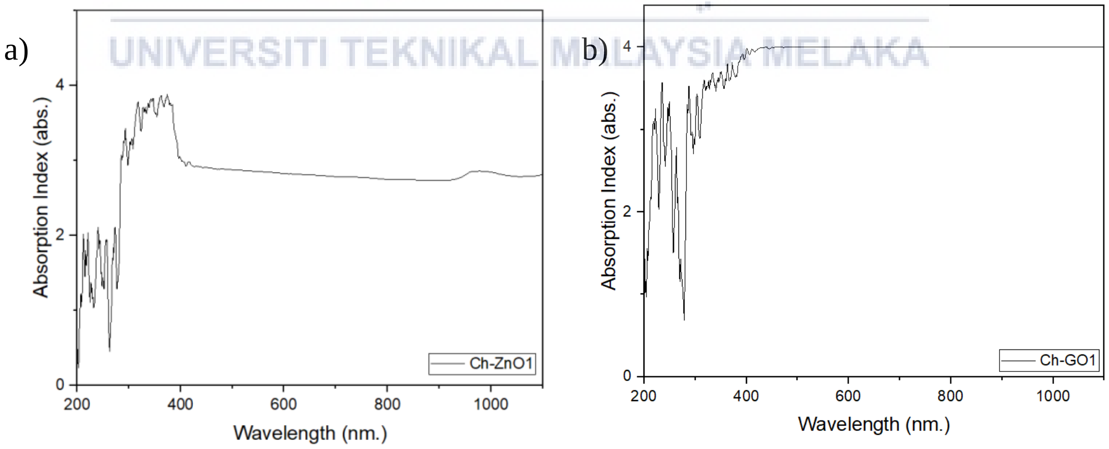

Figure 4.6: Absorption Index (a) Zinc Oxide + Chitosan, (b) Graphene Oxide + Chitosan

Figure 4.6 (a)(b) shows that a group of data from UV-Vis spectroscopy in the form of graph of absorption index. Comparing these 2 sample, graphene oxide + chitosan having the highest absorption value compared to the zinc oxide + chitosan. The higher the absorption index value, the better the material is at absorbing light, which is allowing less light to get through. From absorption index, refractive index can be calculated by using Formula (2) and (3).

$$T_s = 10^{(-A)} \times 100 \qquad (2)$$

$$n = \frac{1}{T_s} + \sqrt{\frac{1}{T_s - 1}} \qquad (3)$$

$T_s = Transmittance\ Index$

$A = Absorption\ Index$

$n = Refractive\ Index$

By applying these two formula, (2) and (3), refractive index can be formed. Refractive index is determined by dividing the speed of light in a vacuum by the speed of light in a second medium with a higher density. The higher the value on the index, the slower light passes through the medium, the more light is deflected, and, ultimately, the more light is bent.

4.2.4 4-Probe Testing

This 4-probe testing usually used to test a thin layer or substrate's sheet resistance in ohms per square by passing current through two outer probes and monitoring the voltage across two inner probes. Figure 4.7 (a)(b)(c) below shows 3 sample that have been deposited on FTO glass and being conducted for 4-probe test.

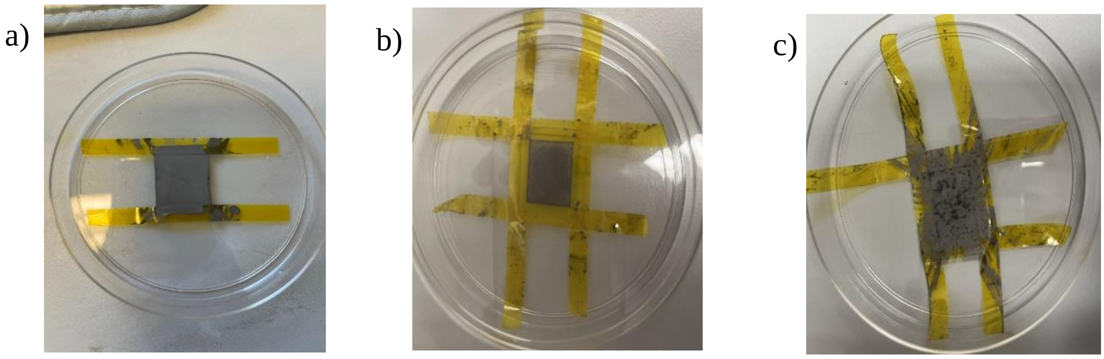

Figure 4.7: (a) Graphene, (b) Graphene-Chitosan (Chemiz.my), (c) Chitosan-Graphene (sample 1)

Testing with four probes was done on top of the glass that had been deposited. The tiny electrodes are placed at the 4 corners and 1 in the middle of the wafer, and electrical resistance between them is measured. Figure 4.8 below shows the area where the glass is being tested. This testing is done in accordance with the area requirements that have been provided.

Figure 4.8: Area of 4-Probe Testing

For each solution that has been deposited on FTO glass, this testing has been carried out five times at different areas. This is conducted to make sure that the data collected to analyze the sample's electrical conductivity is comparable. The 3 samples include, graphene, graphene mixed chitosan from Chemiz.my and graphene mixed with chitosan from sample 1. This composition or mixture is prepared to account for whether or not the conductivity will be impacted by the addition of polymer to a sample or solution. Table 4.4 below shows the experimental value of the 4-probe test on the deposited glass.

Table 4.4: Comparison on conductivity for 3 different samples

Area	**Graphene**			**Graphene-Chitosan (Chemiz.my)**			**Chitosan-Graphene (Sample 1)**		
	Resistivity (kΩ)	Square Resistivity (kΩ)	Resistance (kΩ)	Resistivity (kΩ)	Square Resistivity (kΩ)	Resistance (kΩ)	Resistivity (kΩ)	Square Resistivity (kΩ)	Resistance (kΩ)
Area 1	0.35	3.35	0.43	1.57	11.37	5.25	6.88	21.11	11.43
Area 2	0.42	1.89	0.60	1.30	9.37	2.05	13.28	54.3	21.2
Area 3	0.29	2.72	0.49	2.63	18.79	4.13	10.12	74.7	16.50
Area 4	0.42	3.43	0.44	1.36	9.68	2.14	3.67	26.19	5.62
Area 5	**0.41**	3.35	**0.41**	**1.07**	7.82	**1.68**	**2.41**	17.18	**3.88**

Refer to the table 4.4, the data in Area 5 is the consistent data compared to the other area. Significant differences can be caused by uneven surfaces during testing. Area 5 on top of the FTO glass is the area where the most uniform layer since the spin coating spinning in circle form compared to the other area where there is a possibility of double coating when the spin coater is spinning. This inconsistent value may be caused by the error in human handling while deposited the sample on the spin coating machine.

An electrical resistivity, also known as specific electrical resistance or volume resistivity, ρ, determines how effectively it opposes the flow of electric current. A material that readily permits electric current has a low resistance. Refer to table 4.4, with the addition of chitosan as a polymer into graphene, it effects the resistivity of the sample. Graphene mixed with chitosan (Sample 1) having the highest value of resistivity compared to the graphene mixed with chitosan (Chemiz.my) and the graphene itself which value of 2.41kΩ, 1.07kΩ and 0.41kΩ respectively. It can be concluded that the chitosan mixed with graphene can be good in oppose the current from flow.

4.3 Simulate Chitosan mixed as Electron Transport Layer (ETL) by using OghmaNano.

In this subtopic, the student will discuss about the simulation by applying chitosan in the electron transport layer by using OghmaNano software. Each process result will be shown below.

4.3.1 Simulation by using OghmaNano

All of these simulations will use Sun as the light source with a similar layer of material such as ITO as the contact material, nickel oxide as photocathode or HTL, MaPbI3 as perovskite layer, chitosan mixed as in photoanode or ETL and silver or Ag as a metal contact. In order to study the performance of the chitosan, the chitosan itself will be mixed with zinc oxide and the comparison can be made by changing the chitosan with graphene oxide on ETL side. The thickness for each layer has been set to fixed meanwhile the changes only happen to the electrical parameter and the sample used as the ETL. Table 4.5 shows the performance for each type of solar cell by simulation.

Table 4.5: Performance of simulated organic solar cell using OghmaNano software

Type of Layer	**Zinc Oxide**	**Zinc Oxide + Chitosan**	**Graphene Oxide + Chitosan**
Voc (V)	0.74	0.32	0.65
Jsc (Am-2)	3.85	2.99	4.16
Fill factor (a.u.)	0.79	0.60	0.75
Power Conversion Efficiency (%)	22.51	5.86	20.52

Table 4.5 shows that the performance for each type of sample in term of Voc, Jsc, fill factor and power conversion efficiency. Graphene oxide mixed with chitosan shows the highest value of PCE compared to the zinc oxide mixed with chitosan at which 20.52% and 5.86% respectively. It shows that the graphene mixed chitosan is better to remove the electrons from the perovskite layer and prevent the recombination of holes in the perovskite layer with electrons compared to zinc oxide mixed with chitosan. The PCE of zinc oxide is way higher compared to graphene oxide mixed chitosan at 1.99%.

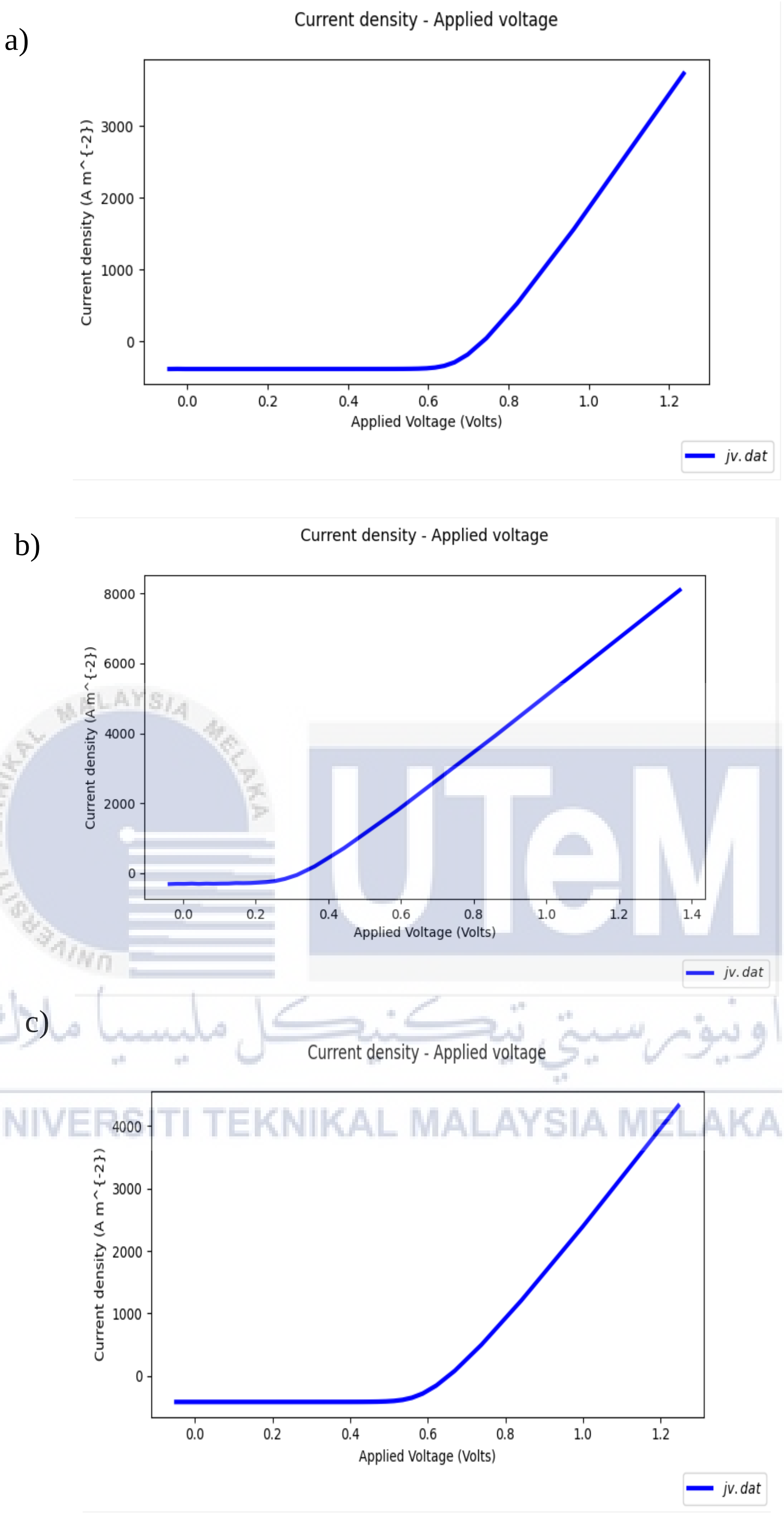

Figure 4.9: Simulation on Jsc curve. (a) zinc oxide as ETL layer, (b) Zinc Oxide mixed Chitosan, (c) Graphene Oxide mixed Chitosan.

Figure 4.9 shows that the Jsc curve for each of the simulation. From the figure above shows that the highest for open-circuit voltage (Voc) when Jsc=0, is on zinc Oxide with 0.74V meanwhile the lowest for open-circuit voltage refer to zinc Oxide + chitosan which only 0.32V. Meanwhile, for the short-circuit current (Jsc) when the Voc=0, the highest short-circuit current is graphene oxide mixed chitosan with 4.16 Am-2. On the other hand, zinc oxide mixed chitosan layer exhibits the lowest short-circuit current compared to all others layer with 2.99 Am-2.

CHAPTER 5

CONCLUSION AND FUTURE WORKS

This chapter was reviewed the project, conclude, sustainable development goals (SDG) and recommend future enhancements for this project. The achievement of this phase has been answered according to the result.

As a conclusion, this project has been providing an overview of work done by doing the synthetization of the chitosan from dried shrimp shell. 2 sample of dried shrimp shell that have been grinding with different in size have achieved that the sample with the range of 1-110µm is the smallest in particle size compared to the sample in range of 100-600µm. The smallest size particle has been chosen to proceed with the synthetization of the chitosan. Next, the synthesis of chitosan started when few parameters have been changed to identify if there is any difference. Three sample of chitosan has been successfully produced. 72% degree of deacetylation was successfully obtained from the synthesis process for Sample 1, compared to the Sample 2 and Sample 3 where it only achieves 70% and 71% degree of deacetylation value respectively.

From FTIR analysis, it shows that all the samples were chitosan but the quality of chitosan individuates the samples. Chitosan with the highest number degree of deacetylation have been choose to mix with graphene oxide and zinc oxide. Chitosan mixed graphene oxide and chitosan mixed zinc oxide have been sent out to UV-Vis testing to gather the value of absorption index. Based on the result, chitosan mixed with Graphene oxide received the highest absorption index compared to zinc oxide which achieved at 4a.u. and 3a.u. respectively which also showed that graphene oxide appears darker and more intensely colored compared to zinc oxide. The higher the absorption index value, the shorter the wavelength to absorb the light intensity.

Furthermore, on the experimental fabrication, three sample have been successfully deposited on the glass and being tested by using spin-coating technique and applying the simulation using Engauge Digitizer and OghmaNano software. Each sample has been designated an area to be tested using 4-probe testing where the areas are on the left, right, top, bottom and in the middle of the FTO glass. The data obtained shows that the middle area of the FTO glass have the have almost equal values compared to other areas which only have slightly difference. Chitosan mixed graphene have the highest value of resistance and resistivity compared to graphene itself with value 3.88kΩ, 0.41kΩ and 2.41kΩ, 0.41kΩ. From experimental fabrication show that the chitosan can increase the impact resistance and their resistivity of the material. For the simulation part, by applying chitosan-graphene oxide in ETL shows that the PCE can reach up to 20.52% compared to zinc oxide in ETL with the thickness of 5nm with 22.51%. Although the obtained data show the performance of chitosan based is lower than zinc oxide based in ETL, chitosan does affect the performance of Perovskite Solar Cell. It can be concluded that the chitosan based into the samples has the potential as an electron transport layer (ETL) despite exhibiting a degraded performance.

5.1 Sustainable Development Goals (SDG)

The Sustainable Development Goals provide a roadmap for building a better, more sustainable future for everyone. In this project, it is more focus on SDG 13 which about the awareness-raising and human, institutional capacity on climate change mitigation, adaptation, impact reduction and early warning. By having this project, SDG 13 can be achieved through education, innovation and can make the required changes to protect the Earth if the climate obligations are followed. The main issue of this project is related to the pollution caused by the disposal of food waste in the fishing sector. Statistically, almost 80,000 tons have been produced every year which can result in pollution. Sometimes this contamination can occur in seafood restaurants that dispose of unfiltered shelled seafood. Additionally, this project is one that does not cost much expenses, using materials that are inexpensive and has a straightforward process, making it a great choice for people of all ages to do. Finally, with this project, shrimp shell waste serves as one of the good examples that can be produced as one of the new polymers that can be employed in a variety of industries, including biomedicine, electronics, agriculture, cosmetics, and many more.

5.2 Future Work

Two suggestions are made for the improvement or continuation of this project, the first of which is to synthesize each PSC layer using chitosan and characterize the outcomes. The next step is to change the parameters or electrical parameters in the OghmaNano software, for instance, changing the thickness of each layer, for the simulation part. It can also be done by using other software programmers, such as Scap1D, and attempting to compare the PCE values of two different software.

REFERENCES

[1] P. Ciambelli, G. La Guardia, and L. Vitale, “Nanotechnology for green materials and processes,” *Stud. Surf. Sci. Catal.*, vol. 179, pp. 97–116, 2019, doi: 10.1016/B978-0-444-64337-7.00007-0.

[2] W. M. Sarhan, A. N. Alkhateeb, K. D. Omran, and F. H. Hussein, “Effect of temperature on the efficiency of the thermal cell,” *Asian J. Chem.*, vol. 18, no. 2, pp. 982–990, 2006.

[3] S. I. Mohammed, “Advantages of Green Technology to Mitigate the Environment Problems,” *IOP Conf. Ser. Earth Environ. Sci.*, vol. 779, no. 1, 2021, doi: 10.1088/1755-1315/779/1/012133.

[4] Y. Rong *et al.*, “Challenges for commercializing perovskite solar cells,” *Science (80-.).*, vol. 361, no. 6408, 2018, doi: 10.1126/science.aat8235.

[5] K. Divya and M. S. Jisha, “Chitosan nanoparticles preparation and applications,” *Environ. Chem. Lett.*, vol. 16, no. 1, pp. 101–112, 2018, doi: 10.1007/s10311-017-0670-y.

[6] M. J. Naughton *et al.*, “Efficient nanocoax-based solar cells,” *Phys. Status*

Solidi - Rapid Res. Lett., vol. 4, no. 7, pp. 181–183, 2010, doi: 10.1002/pssr.201004154.

[7] K. Ranabhat, L. Patrikeev, A. A. evna Revina, K. Andrianov, V. Lapshinsky, and E. Sofronova, “An introduction to solar cell technology,” *J. Appl. Eng. Sci.*, vol. 14, no. 4, pp. 481–491, 2016, doi: 10.5937/jaes14-10879.

[8] G. Ali, M. Omar, A. K. Khan, and M. Faisal Nadeem, “Recent Challenges of Solar Cell Technologies; A Critical Analysis,” *RAEE 2018 - Int. Symp. Recent Adv. Electr. Eng.*, pp. 1–5, 2018, doi: 10.1109/RAEE.2018.8706887.

[9] H. S. Jung and N. G. Park, “Perovskite solar cells: From materials to devices,” *Small*, vol. 11, no. 1, pp. 10–25, 2015, doi: 10.1002/smll.201402767.

[10] V. Gonzales-Pedro, E. J. Juarez-Perez, E. Arsyad, Waode-SukmawaM.Barea, F. Fabregat-Santiago, I. More-Sero, and J. Bisquert, “General Working Principles of CH 3 NH 3 PbX 3 Perovskite Solar Cells,” *Nano Lett.*, vol. 14, no. 2, pp. 888–893, 2014.

[11] S. Yun, X. Zhou, J. Even, and A. Hagfeldt, “Theoretical Treatment of CH3NH3PbI3 Perovskite Solar Cells,” *Angew. Chemie - Int. Ed.*, vol. 56, no. 50, pp. 15806–15817, 2017, doi: 10.1002/anie.201702660.

[12] D. Zhou, T. Zhou, Y. Tian, X. Zhu, and Y. Tu, “Perovskite-Based Solar Cells: Materials, Methods, and Future Perspectives,” *J. Nanomater.*, vol. 2018, 2018, doi: 10.1155/2018/8148072.

[13] N. A. Salleh, S. Kheawhom, and A. A. Mohamad, “Chitosan as biopolymer binder for graphene in supercapacitor electrode,” *Results Phys.*, vol. 25, p.

104244, 2021, doi: 10.1016/j.rinp.2021.104244.

[14] L. Zhang, L. Chai, Q. Qu, L. Zhang, M. Shen, and H. Zheng, “Chitosan, a new and environmental benign electrode binder for use with graphite anode in lithium-ion batteries,” *Electrochim. Acta*, vol. 105, pp. 378–383, 2013, doi: 10.1016/j.electacta.2013.05.009.

[15] Â. A. S. Oliveira *et al.*, “One-step synthesis of LaNiO3 with chitosan for dry reforming of methane,” *Int. J. Hydrogen Energy*, vol. 43, no. 20, pp. 9696–9704, 2018, doi: 10.1016/j.ijhydene.2018.03.212.

[16] C. Chen, S. H. Lee, M. Cho, J. Kim, and Y. Lee, “Cross-Linked Chitosan as an Efficient Binder for Si Anode of Li-ion Batteries,” *ACS Appl. Mater. Interfaces*, vol. 8, no. 4, pp. 2658–2665, 2016, doi: 10.1021/acsami.5b10673.

[17] G. M. Mathew *et al.*, “Sustainable and eco-friendly strategies for shrimp shell valorization,” *Environ. Pollut.*, vol. 267, p. 115656, 2020, doi: 10.1016/j.envpol.2020.115656.

[18] X. Yang, Y. Tu, L. Li, S. Shang, and X. M. Tao, “Well-dispersed chitosan/graphene oxide nanocomposites,” *ACS Appl. Mater. Interfaces*, vol. 2, no. 6, pp. 1707–1713, 2010, doi: 10.1021/am100222m.

[19] A. Boscá, J. Pedrós, J. Martínez, and F. Calle, “Method for extracting relevant electrical parameters from graphene field-effect transistors using a physical model,” *J. Appl. Phys.*, vol. 117, no. 4, pp. 1–7, 2015, doi: 10.1063/1.4906972.

[20] P. You, Z. Liu, Q. Tai, S. Liu, and F. Yan, “Efficient Semitransparent Perovskite Solar Cells with Graphene Electrodes,” *Adv. Mater.*, vol. 27, no. 24,

pp. 3632–3638, 2015, doi: 10.1002/adma.201501145.

[21] P. R. Sivashankari and M. Prabaharan, “Deacetylation modification techniques of chitin and chitosan,” *Chitosan Based Biomater.*, vol. 1, no. October 2020, pp. 117–133, 2017, doi: 10.1016/B978-0-08-100230-8.00005-4.

APPENDICES

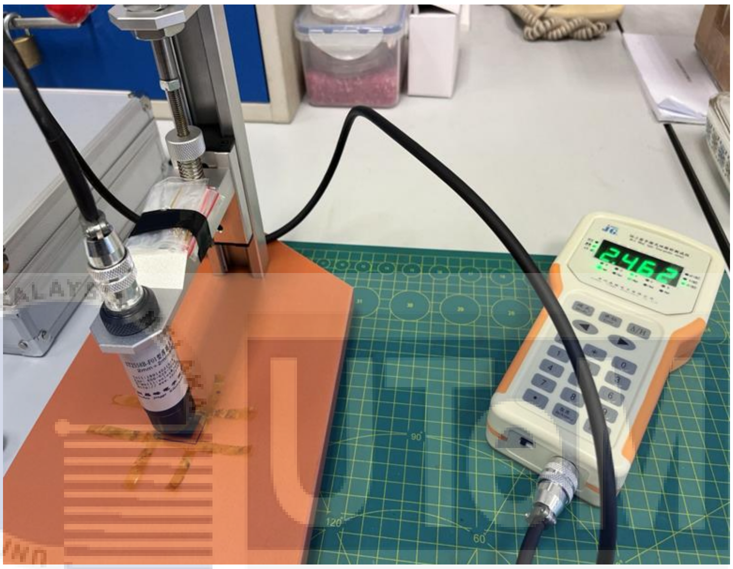

Figure 5.1: 4-Probe Testing for conductivity test

Figure 5.2: UV-Vis Testing to get the Absorption Index of the sample